HHS Public Access

Author manuscript

J Neurosci Methods. Author manuscript; available in PMC 2017 May 01.

Published in final edited form as:

J Neurosci Methods. 2016 May 1; 264: 136–152. doi:10.1016/j.jneumeth.2016.02.021.

Determining Synaptic Parameters Using High-Frequency Activation

Monica S. Thanawala[a,b] and **Wade G. Regehr**[a,*]

Wade G. Regehr: wade_regehr@hms.harvard.edu

[a]Department of Neurobiology, Harvard Medical School, Boston MA

Abstract

Background—The specific properties of a synapse determine how neuronal activity evokes neurotransmitter release. Evaluating changes in synaptic properties during sustained activity is essential to understanding how genetic manipulations and neuromodulators regulate neurotransmitter release. Analyses of postsynaptic responses to high-frequency stimulation have provided estimates of the size of the readily-releasable pool (RRP) of vesicles (N_0) and the probability of vesicular release (p) at multiple synapses.

New Method—Here, we introduce a model-based approach at the calyx of Held synapse in which depletion and the rate of replenishment (R) determine the number of available vesicles, and facilitation leads to a use-dependent increase in p when initial p is low.

Results—When p is high and R is low, we find excellent agreement between estimates based on all three methods and the model. However, when p is low or when significant replenishment occurs between stimuli, estimates of different methods diverge, and model estimates are between the extreme estimates provided by the other approaches.

Comparison with Other Methods—We compare our model-based approach to three other approaches that rely on different simplifying assumptions. Our findings suggest that our model provides a better estimate of N_0 and p than previously-established methods, likely due to inaccurate assumptions about replenishment. More generally, our findings suggest that approaches commonly used to estimate N_0 and p at other synapses are often applied under experimental conditions that yield inaccurate estimates.

Conclusions—Careful application of appropriate methods can greatly improve estimates of synaptic parameters.

Keywords

Synaptic transmission; Calyx of Held; Readily-releasable pool; Release probability

Goldenson 308, Department of Neurobiology, Harvard Medical School, 220 Longwood Avenue, Boston, MA 02115. Tel: 617 432 0450, fax: 617 432 1639.

bPresent address: Department of Chemistry and Chemical Biology, Harvard University, Cambridge MA

The authors declare no competing financial interests.

1. Introduction

The number of vesicles in the readily-releasable pool (RRP) and the probability of release (p) are fundamental properties of synapses that are used to characterize their basal characteristics and to describe how they are modified by activity, neuromodulators, and genetic manipulations. One way to evaluate RRP size and p is to use a powerful non-physiological means of liberating all vesicles in the RRP, such as prolonged presynaptic voltage steps, photolytic presynaptic calcium release, or applications of hypertonic sucrose, and then using capacitance measurements or postsynaptic voltage-clamp recordings to quantify the RRP (Schneggenburger et al. 2002; Zucker and Regehr 2002; Schneggenburger and Neher 2005). These approaches have all provided important insights into synaptic transmission, but for technical reasons, they cannot be readily applied to many types of synapses. Moreover, the pool of vesicles that exocytoses in response to these non-physiological stimuli may not be equivalent to the pool that can be released through physiologically-relevant action potential stimuli (Neher 2015). To overcome these limitations, a second class of approaches has been developed that uses synaptic currents evoked by high frequency stimulation to estimate p and RRP. Such approaches have the advantage that they are based on synaptic responses evoked under physiological conditions and can be readily applied to many types of synapses.

Here we evaluate different methods that are used to estimate synaptic parameters from responses evoked by high-frequency stimulation. A basic framework has been developed to understand how neurotransmitter is released in response to rapid firing. It is thought that release depends on the size of the RRP (comprised of a number of vesicles, N_0) and the probability of an action potential causing a vesicle to fuse (p). The number of vesicles released by an action potential is equal to $p \times N_0$ (Liley and North 1953). At synapses with a high initial p, repetitive activation rapidly depletes the RRP and reduces the amount of neurotransmitter release per action potential (Elmqvist and Quastel 1965). As depletion occurs, a synapse relies on vesicles from a recycling pool of vesicles to replenish the RRP.

Several methods have been developed to determine synaptic properties that are based on this simple framework. The most widely used method to characterize synaptic properties uses high-frequency stimulation to evoke EPSCs (Fig. 1A). According to this approach, rapid stimulation depletes the RRP until the remaining responses rely on the replenishment of the readily-releasable pool. A plot of the cumulative EPSC versus stimulus number has a rapidly changing component during which the RRP is depleted, followed by a linear component once the EPSC reaches a constant amplitude (Fig. 1B, Table 1). N_0 is estimated by extrapolating the linear phase back to the y-axis in order to account for replenishment. This quantity is in units of current, and corresponds to a number of vesicles released when divided by the quantal size, q. Then p is determined as p=EPSC$_0$/N_0 (Schneggenburger et al. 1999). This method, as well as a variation that uses presynaptic capacitance changes instead of postsynaptic responses, has been applied to characterize synaptic transmission at a variety of synapses, including the calyx of Held, excitatory and inhibitory cultured hippocampal synapses, and the *Drosophila* neuromuscular junction (Schneggenburger et al. 1999; Moulder and Mennerick 2005; Stevens and Williams 2007; Fioravante et al. 2011; Liu et al.

2014; Gaviño et al. 2015; Müller et al. 2015). The same data can also be used to estimate synaptic parameters using an approach developed by Elmqvist and Quastel (Elmqvist and Quastel 1965; Ruiz et al. 2011) that relies on a different set of assumptions (Fig. 1C, Table 1). The Elmqvist and Quastel (EQ) method is less widely used than the train method, but has still been applied at multiple synapses. It relies primarily on EPSCs early in the train and assumes that the decrease in EPSC amplitudes during high-frequency stimulation is a result of depletion of a homogenous pool of synaptic vesicles that comprise the RRP. With this method, a linear fit to the earliest few points of a plot of the EPSC amplitude versus the cumulative EPSC is used to estimate the size of the RRP, and p=EPSC$_0$/N_0. The data can also be analyzed with what we refer to as the decay method (Ruiz et al. 2011), which has not been used extensively. According to this approach, the amplitude of the nth synaptic response evoked by a train is EPSC$_n$=EPSC$_0$(1−p)^n + C (C is a constant). An exponential fit to the EPSC amplitude as a function of stimulus number is used to estimate p, and N_0=EPSC$_0$/p (Fig. 1D).

All of these methods rely on assumptions that are not valid under all conditions, which can compromise their accuracy in estimating synaptic parameters (Table 1). The EQ and decay methods assume that the effects of replenishment are small and can be ignored, but it is not always clear if this is valid for typical experimental conditions. Although the train method does consider replenishment, it assumes constant replenishment throughout a stimulus train. In fact, replenishment could scale with the availability of empty release sites (Wesseling and Lo 2002) and accelerate with elevation of presynaptic calcium levels (Kusano and Landau 1975; Dittman and Regehr 1998; Wang and Kaczmarek 1998; Sakaba and Neher 2001a; Hosoi et al. 2007), which could lead to underestimates of RRP size (but see Neher, 2015). With regard to p, the train method is most flexible, in that it allows for changes in p throughout the stimulus train and heterogeneity of p among individual vesicles in the RRP. In contrast, the EQ and decay methods assume uniform p that remains constant throughout a stimulus train. However, p does not remain constant at facilitating synapses, and p may be non-uniform at many synapses (Dobrunz and Stevens 1997; Sakaba and Neher 2001b; Meinrenken et al. 2002; Trommershäuser et al. 2003; Moulder and Mennerick 2005; Schneggenburger et al. 2012).

In this study, we compare estimates of synaptic parameters at the calyx of Held synapse based on four approaches: the train method (Schneggenburger et al. 1999), the EQ method (Elmqvist and Quastel 1965), the decay method (Ruiz et al. 2011), and fitting to a depletion-based model. There is good agreement between the estimates obtained with all approaches when p is high, R is low, and stimulus frequency is high. When this is not the case, model estimates of RRP size are greater than those of the train and decay methods but less than those of the EQ method. The values obtained with these four methods can differ significantly under non-ideal conditions and suggest that care is necessary in choosing an approach to analyze such data. Our findings suggest that under non-ideal conditions, a depletion-based model provides better estimates, because the model is based on a more accurate description of replenishment of the RRP than is implicit in the in the train, decay, and EQ methods. We also use the depletion model to explore the effects of changes in p, replenishment rate, and firing frequency on the ability of linear extrapolation estimates to accurately measure N_0 and p. We find that the train method and EQ method perform best in

moderate to high *p* conditions with relatively low replenishment rates and high firing frequencies. These studies provide insight into the optimal approaches to estimate synaptic parameters at the calyx of Held, advocate for simultaneous use of multiple approaches at a given dataset, and have important implications for the study of other synapses.

2. Materials and Methods

2.1 Animals and Preparation of Brain Slices

All animals used were wildtype mice (BL6C57/6J, Jackson Laboratories), postnatal day P11–14 of either sex. All animal handling and procedures abided by the guidelines of the Harvard Medical Area Standing Committee on Animals. Mice were deeply anesthetized with isoflurane and killed by decapitation. Transverse 200-μm-thick slices were cut from the brainstem containing the medial nucleus of the trapezoid body (MNTB) with a vibratome slicer. Brains were dissected and sliced at 4°C in a solution consisting of the following (in mM): 125 NaCl, 25 $NaHCO_3$, 1.25 NaH_2PO_4, 2.5 KCl, 0.1 $CaCl_2$, 3 $MgCl_2$, 25 glucose, 3 myo-inositol, 2 Na-pyruvate, 0.4 ascorbic acid, continuously bubbled with 95% O_2/5% CO_2 (pH 7.4). Slices were incubated at 32°C for 20 min in a bicarbonate-buffered solution composed of the following (in mM): 125 NaCl, 25 $NaHCO_3$, 1.25 NaH_2PO_4, 2.5 KCl, 2 $CaCl_2$, 1 $MgCl_2$, 25 glucose, 3 myo-inositol, 2 Na-pyruvate, 0.4 ascorbic acid, continuously bubbled with 95% O_2/5% CO_2 (pH 7.4). For experiments conducted in an external calcium concentration other than 2 mM, slices were incubated in a solution similar to that above but with varying $CaCl_2$ and $MgCl_2$ concentrations. The concentration of $CaCl_2$ added to that of $MgCl_2$ was always equal to 3 mM when $Ca_e \leq 2$ mM. For experiments with $Ca_e = 3$ mM and 4 mM, $[Mg^{2+}]$=0.1 mM.

2.2 Electrophysiology

Slices were transferred to a recording chamber at room temperature (~25 °C). During recordings, the standard perfusion solution consisted of the bicarbonate-buffered solution (see above) with 1 μM strychnine and 25 μM bicuculline to block inhibitory synaptic transmission. 1 mM kynurenic acid and 0.1 mM cyclothiazide (Tocris Bioscience/R&D Systems, Minneapolis, MN) were also added to block AMPA receptor saturation and desensitization, respectively. The recording chamber was superfused at 1–3 ml/min with this external solution. Whole-cell postsynaptic patch-clamp recordings were made from visually identified cells in the MNTB region using glass pipettes of 2–3 MΩ resistance, filled with an internal recording solution of the following (in mM): 110 CsCl, 35 CsF, 10 EGTA, 10 HEPES, 2 QX-314, pH: 7.2, 315–320 mOsm. Series resistance (R_s) was compensated by up to 60% and the membrane potential was held at −60 mV. Excitatory postsynaptic potentials (EPSCs) were evoked by stimulating presynaptic axons with a bipolar stimulating electrode placed midway between the medial border of the MNTB and the midline of the brainstem. A Multiclamp 700A (Axon Instruments/Molecular Devices, Union City, CA) amplifier was used. Recordings were digitized at 20 kHz with an ITC-18 A/D converter (Instrutech, Port Washington, NY) using custom procedures (written by M.A. Xu-Friedman) in IgorPro (Wavemetrics, Lake Oswego, OR) and filtered at 8 kHz. Access resistance and leak current were monitored and experiments were rejected if either parameter changed significantly.

Recordings were performed under a variety of conditions in order to modulate initial p. The first manipulation was to include different concentrations of extracellular calcium (Ca_e, 1–4 mM) in the recording solution. In other experiments, pharmacological agents were applied in standard (2 mM) external Ca^{2+}. $NiCl_2$ (100 μM) was applied to block R-type calcium channels (Soong et al. 1993; Schneider et al. 1994; Zamponi et al. 1996), which has been shown to be effective at the calyx of Held (Wu et al. 1998, 1999). ω-Aga-IVA (50 nM) was used to block P-type calcium channels (Iwasaki and Takahashi 1998). Baclofen (100 μM), a $GABA_B$ receptor agonist, was used to inhibit voltage-gated calcium channels (Takahashi et al. 1998), and CGP 55845 (20 μM), a $GABA_B$ receptor antagonist, was used to alleviate tonic inhibition of voltage-gated calcium channels due to ambient levels of GABA in the slice.

2.3 Data Analysis

The effective size of the RRP and p were calculated using several techniques. The methods for the train and EQ methods are also described in a previous work (Thanawala and Regehr 2013). For all methods, EPSC amplitudes were measured by subtracting the baseline current just preceding an EPSC from the subsequent peak of the EPSC. For the RRP_{train} technique, EPSC amplitudes were then summed throughout the train stimulus to give a cumulative EPSC curve. For a detailed explanation of the general theory behind this method, see Neher, 2015. In this study, a straight line was fitted to the final fifteen points of the cumulative EPSC and back-extrapolated to the y-axis. The y-intercept corresponds to RRP_{train}, and $p_{train}=EPSC_0/RRP_{train}$, as previously described (Schneggenburger et al., 1999). An example showing how RRP_{train} and p_{train} are measured from this plot is shown in Fig. 1B, and example plots of simulated data are shown in Fig. 1E, H, and K to illustrate how changes in N_0, p, and R affect the shape of the cumulative EPSC, respectively. Data was simulated for these plots using a model that is discussed later in Methods. In these simulations, f=1, such that there is no facilitation.

To apply the EQ method (Elmqvist and Quastel, 1965), peak EPSC amplitudes were plotted versus the cumulative EPSC. A recent publication provides an excellent explanation of the theory behind the EQ method (Neher 2015). Specifically, in this study a line was fitted to four points whose decrement is primarily determined by depletion of the RRP. If the paired-pulse ratio (PPR) was less than or equal to 1, the first four points were used in the linear fit. If the PPR was greater than 1, the second through fifth points were used in the linear fit. This was to minimize the already-minor effects of facilitation at this synapse on our estimates. The x-intercept of the linear fit corresponds to RRP_{EQ}. Additionally, the value of p is estimated according to $p_{EQ}=EPSC_0/RRP_{EQ}$. An example showing how RRP_{EQ} and p_{EQ} are measured from this plot is shown in Fig. 1C, and example plots of simulated data are shown in Fig. 1F, I, and L to illustrate how changes in N_0, p, and R affect the plots used for this method. For some particularly low p examples, the linear fit yielded negative values for RRP_{EQ}, which indicates failure of the method. We excluded these data points.

For the decay method, peak EPSC amplitudes were plotted versus stimulus number. A single exponential function of the form $y = A(1-e^{-1/\lambda})$, where A is a constant and λ corresponds to stimulus number, was fitted from the largest EPSC through the 40^{th} EPSC in response to a

train stimulus. This method ignores replenishment, and as such, the decay constant λ can be used to directly estimate p_{decay}. In order to correct for the small effects of facilitation on the first synaptic response, the exponential fit was back-extrapolated to the y-axis, and the amplitude of the curve-fit at x=0 was compared to the actual amplitude of the first EPSC ($EPSC_0$). A facilitation factor, f, was computed in which $f = EPSC_0(fit)/EPSC_0$ (Fig. 3E). The value of p_{decay} was then estimated as $p_{decay}=(1-e^{-1/\lambda})/f$ and $RRP_{decay}=EPSC_0/p_{decay}$. An example showing how RRP_{decay} and p_{decay} are measured is shown in Fig. 1D, and example plots of simulated data are shown in Fig. 1G, J, and M to illustrate how changes in N_0, p, and R affect the plots used for this method. Additionally, we estimated RRP size and p without the correction for facilitation. This estimates the steady-state value of p from the decay constant of EPSCs in response to a train, beginning with the largest EPSC as previously, such that $p_{decay(ss)}=(1-e^{-1/\lambda})$ and $RRP_{decay(ss)}=EPSC_0/p_{decay(ss)}$. For only one very low p synapse, a single exponential function could not be fitted to the data, and this cell was excluded.

Data analysis was performed using routines that were custom written in IgorPro. Linear and exponential curve fitting was performed using a built-in least-squares curve fitting application in IgorPro.

2.4 Modeling and simulations

We simulated responses during trains with a modified depletion model, with replenishment of vesicles into the RRP determining occupancy of the RRP and thus synaptic response amplitudes in response to a high-frequency stimulus. A number of studies at the calyx of Held and other synapses implement similar models (Zucker and Regehr 2002; Neher and Sakaba 2008; Ruiz et al. 2011; Thanawala and Regehr 2013). We refer to the version presented here as the NpRf model because it uses 4 parameters to describe release during trains: N_0, the initial size of the RRP prior to stimulation; p, the initial probability of release for the first EPSC in the train; R, the rate of replenishment of the RRP from a reserve pool; and f, a factor that accounts for facilitation. The parameter R is a rate constant with a dimension 1/stimulus rather than 1/s, and as such describes the amount of replenishment between stimuli. According to this model the number of vesicles in the RRP, $N(t)$, is use-dependent and time-dependent, and in the absence of stimulation $N=N_0$. The probability of release is also use-dependent. It starts at an initial value of p and increases between the first and second stimulus to a steady-state value of pf that persists throughout the stimulus train. For the initial EPSC:

$$EPSC_0 = pN_0 \quad (1)$$

For the second stimulus at time t_1 which results in $EPSC_1$:

$$N_1 = N_0\,(1-p+pR) \quad (2)$$

$$EPSC_1 = pfN_1 \quad (3)$$

and the recovery of the RRP between the first and second stimuli is given by:

$$R_1 = RpN_0 \quad (4)$$

For all subsequent EPSCs (stimulus number n>1)

$$N_n = N_{n-1}(1 - pf - R + pfR) + N_0 R \quad (5)$$

$$EPSC_n = pfN_n \quad (6)$$

The recovery of the RRP between the stimulus n−1 and stimulus n is given by:

$$R_n = N_{n-1}R(pf - 1) + N_0 R \quad (7)$$

For this model, recovery of the RRP depends upon the occupancy of the RRP, and there is substantially more recovery between stimuli late in the train. When the model is fitted to data, the average time course of recovery is not used; instead, our fitting function determines the rate of replenishment per stimulus that fits the data.

To apply the NpRf model to real data, we first determine f, which is the same facilitation factor calculated for the decay method. When PPR<1, all forty EPSC amplitudes are used to generate an exponential fit and f = $EPSC_0$(fit)/$EPSC_0$. If the PPR>1, the exponential function is fit to EPSC amplitudes from the second stimulus through the end of the train. When p is large, f=1, and as p becomes smaller f becomes larger. This provides the simplest means of accounting for facilitation and extends the applicability of the model to conditions where p is low and a depletion model that lacks facilitation is inadequate. We then fit the synaptic responses evoked by a train to the prediction of the NpRf where N_0, p, and R are freely varying parameters. This procedure finds optimal output values using the Levenberg-Marquardt algorithm, which is a commonly used method for solving non-linear least-squares problems.

For all simulations (Figs. 6–8), facilitation is omitted such that f=1. To determine the extent of recovery between stimuli our simulations with different train frequencies (Fig. 8), we determined the time course of recovery from depression induced by 100 Hz stimulation. This was done by depleting the RRP with a stimulus train of at least 25 stimuli and then varying the time interval elapsed before the next stimulus (see Fig. S1). We fitted this data with a double-exponential function to estimate the amount of replenishment that would occur between stimuli at different frequencies, which yielded the following function:

$$EPSC_{norm}(\Delta t) = 1 - 0.246e^{\left(\frac{-\Delta t}{185\ ms}\right)} - 0.697e^{\left(\frac{-\Delta t}{2900\ ms}\right)} \quad (8)$$

in which $EPSC_{norm}$ represents the steady-state EPSC normalized to the amplitude of the first EPSC in a stimulus train ($EPSC_0$), and Δt represents the interstimulus interval for a given stimulus frequency (Fig. S1). Equations 1–7 can then be used to simulate synaptic responses as a function of the parameters, N_0, p, and R, with f held equal to one as described

previously. See Online Supplemental Material for Igor code to simulate synaptic responses and to apply the NpRf model to real data (Appendix 1).

2.5 Online Supplemental Material

One supplemental figure (Fig. S1) is included that shows data characterizing the time course of recovery from depression at the calyx of Held synapse under standard recording conditions. Appendix 1 provides Igor code for the NpRf model and simulations of postsynaptic responses.

3. Results

To assess the performance of the two linear extrapolation methods that are most widely used to determine synaptic parameters at high p synapses, we compared their estimates of synaptic parameters for 100 Hz trains evoked at the calyx of Held synapse. Synaptic responses were measured under a variety of conditions to obtain data for a wide range of p. Synaptic responses used for these analyses are mostly from a previous study (Thanawala and Regehr 2013), and the data set has been augmented with additional experiments.

Estimates of RRP_{EQ} tended to be larger than RRP_{train} (Fig. 2A, B), and the discrepancy between the two measures was more pronounced under low p conditions (Fig. 2C, D). In conditions that severely reduce EPSC amplitudes, there are substantial discrepancies between the methods. Plots of RRP_{train}/RRP_{EQ} vs. p_{EQ} revealed good agreement between RRP_{EQ} and RRP_{train} when p is high, but estimates diverged considerably when p <0.2.

The differences between the estimates of synaptic properties by these two mechanisms are readily explained by considering the assumptions that underlie these approaches. An implicit assumption of the train method is that the RRP is replenished at a constant rate per terminal throughout the train. Experimental evidence suggests that this is not the case, because the rate of replenishment depends on the number of *empty* release sites. This suggests that as the occupancy of the RRP decreases during high-frequency stimulation, there are more empty release sites into which vesicles can be loaded, resulting in faster replenishment than occurred in the beginning of the train. As a result, the extrapolation is erroneous and the RRP size is underestimated. In contrast, the EQ method (Fig. 1C) disregards replenishment (Elmqvist and Quastel 1965). This assumption leads to an overestimate of RRP size. Thus, RRP_{train} underestimates RRP size and RRP_{EQ} overestimates RRP size, which is consistent with our observation that RRP_{train} is consistently smaller than RRP_{EQ}.

Additionally, neither linear extrapolation technique provides a direct measure of p; rather, the amplitude of the first EPSC is divided by the estimated RRP size to give an estimate of p. $p_{train} = EPSC_0/RRP_{train}$, and $p_{EQ} = EPSC_0/RRP_{EQ}$. Since these indirect measures of p are inversely related to the estimate of RRP size, it makes sense that p_{train} is consistently larger than p_{EQ} for both altered Ca_e and for pharmacological manipulations of calcium entry (Fig. 2E, F). The discrepancies between p_{train} and p_{EQ} are minor under high p conditions, but become substantial below p<0.2, a common value for many other CNS synapses (Fig. 2G, H).

We sought to measure p using a method that does not rely on estimating RRP size. We reasoned that the decay of EPSC amplitudes during high-frequency firing can be used to provide a direct measure of p under high p conditions. In order for this method to work, there must be a single pool of vesicles with uniform p that is depleted fairly rapidly due to repetitive presynaptic firing. If this is the case, then EPSC amplitudes will decay exponentially according to the equation $EPSC_n/EPSC_0=e^{(-n/\lambda)}$, where n is the stimulus number and λ is the decay constant of a single-exponential fit to EPSC amplitudes throughout a train. If the decrement is due to depletion and there is no significant replenishment, then it should be possible to estimate p directly using $p=1-e^{(-1/\lambda)}$. It is difficult to apply this approach if $p>0.5$ because the decrement in the EPSC is so rapid that λ is less that a single stimulus, as well as if $p<0.01$, since λ is more than 100 stimuli (Fig. 3A). Another potential complication is that at the calyx of Held there appear to be high and low p vesicles for release driven by prolonged presynaptic voltage steps or calcium increases (Sakaba and Neher 2001a; Trommershäuser et al. 2003; Wölfel et al. 2007; Chen et al. 2015), but it is not known if low p vesicles contribute to AP-evoked release. If high and low p vesicles both contribute to release evoked by 100 Hz trains, then EPSC amplitudes would decay with a double exponential amplitude ($EPSC_n/EPSC_0=Ae^{(-n/\lambda 1)}+ Be^{(-n/\lambda 2)}$, $p_1=1-e^{(-1/\lambda 1)}$ and $p_2=1-e^{(-1/\lambda 2)}$). This predicts that if there are both high and low p synapses, the EPSC decay as a function of stimulus number cannot be approximated by a single exponential decay, as illustrated for a simplified example (lacking replenishment) in which half of the vesicles in the RRP have $p=0.3$ and the other half have $p=0.03$ (Fig. 3B). As in Fig. 3C, we find that the EPSC amplitudes are well approximated by a single exponential decay, which suggests that release due to action potentials is primarily mediated by a population of vesicles with similar release probability. Further, the PPRs for an interstimulus interval of 10 ms conform well to a line equal to $1-p$ when p is greater than 0.2. This suggests that the amplitudes of EPSCs early in a stimulus train are primarily determined by depletion of a readily-releasable pool of vesicles for synapses that exhibit moderate to high p (Fig. 3D). This would likely not be true for longer interstimulus intervals, because replenishment would bring the occupancy of the RRP closer to its initial state. The data deviate from the $1-p$ line for $p_{train}<0.2$, the point at which facilitation becomes somewhat noticeable, although the amplitude of facilitation is still quite small. This suggests that estimates of p from the decay of EPSC amplitudes will probably be inaccurate under low p conditions as a result. To extend the value of using the decay of EPSC amplitudes to understand data from the calyx of Held synapse, we decided to calculate a facilitation factor, f, to adjust for the facilitation observed between the first and second stimulus. For each cell, we performed a single-exponential curve fit to the plot of EPSC amplitude versus stimulus number, beginning the fit with the largest EPSC. In almost every case, either the first or second EPSC was the largest in the 40-stimulus action potential train. We backextrapolated this curve to the y-axis (Fig. 3E). The facilitation factor, f, equals the amplitude of the curve fit at the y-axis divided by the actual amplitude of $EPSC_0$ (Fig. 3F). We reasoned that the estimate of p obtained from the single-exponential fit (with p that increased during the train by facilitation, or steady-state p) would be greater than the initial value of p during the first action potential by a factor of f. We therefore divided this estimate by f to calculate p_{decay}, which is our estimate of initial p.

We apply the decay method data obtained from varying Ca_e and from pharmacological manipulation of calcium entry to provide many data points covering a wide range of values of initial release probability (from p<0.1 to almost p=0.6, depending on the estimation method used). Plots of p_{decay} versus the two established linear extrapolation methods of estimating p show reasonable agreement between p_{decay} and p_{train} (Fig. 3G) as well as between p_{decay} and p_{EQ} (Fig. 3H). The values for $p_{decay(ss)}$, which are not corrected for facilitation (see **Methods**), are likely to reflect the steady-state of p, display the same trends. A plot of p_{decay}/p_{train} vs. p_{train} reveals that when p_{train} is below 0.2, the agreement between the methods is poor, which is also true for $p_{decay(ss)}$ (Fig. 3I). A comparison to the EQ method similarly reveals the most considerable disagreement between the two methods when p_{EQ} is below 0.2. Under these conditions, p_{decay} and $p_{decay(ss)}$ are generally larger than p_{train} (Fig. 3J). These findings suggest that the amplitude of EPSCs evoked during the train do indeed provide information about p, but that when p<0.2 the methods provide different estimates of synaptic parameters.

These discrepancies may make sense in light of the fact that these methods are based on assumptions about replenishment that are too simple, as discussed previously (Table 1). A comparison of the estimates of the EQ and train methods with the exponential fit method is useful because they are expected to provide estimates of RRP that bracket the actual RRP (Thanawala and Regehr 2013). Our analyses show that when p>0.4, any of the three methods outlined here are likely to provide similar results. For more moderate p between 0.2 and 0.4, the results may be somewhat different, and for p<0.2 the results are likely to differ dramatically.

In order to assess the performance of existing methods and to develop an approach that allows more reliable determination of synaptic parameters, we developed a simple model of synaptic transmission at the calyx of Held that incorporates known properties of replenishment. In this model, replenishment is dependent on the number of empty release sites and thus is not constant during the train. This is based on our experimental observation that more recovery from depression occurs when the extent of depletion is greater. The model has four parameters: the size of the RRP (N_0); the probability of release (p), the rate of replenishment of the readily releasable pool from the recycling pool (R), and a facilitation factor (f) which was introduced in Fig. 3. It has similarities to a number of previous models that have been advanced to describe synaptic properties (Kusano and Landau 1975; Abbott et al. 1997; Tsodyks and Markram 1997; Dittman et al. 2000; Cartling 2002; Yang and Xu-Friedman 2008; Ruiz et al. 2011; Hennig 2013). We call this model the NpRf model.

Our model uses an iterative curve-fitting function (see Methods) in which N_0, p, and R, are optimized after determination of f (see Methods). Importantly, the parameter R has a fixed value such that the rate of replenishment per empty site in the RRP is fixed, while the occupancy of the RRP can change throughout a stimulus train. We use this model to directly determine these four synaptic parameters from synaptic responses evoked by a stimulus train. The use of the model is illustrated in Fig. 4 in which the performance of the model is compared to train and EQ methods. As shown for a high p synapse (p_{NpRf}=0.38), the model approximates the cumulative EPSC and the EPSC amplitudes well (Fig. 4A–C, *black line*). There was remarkably good agreement in the estimates of RRP for the different methods

(RRP_{train}= 17.0 nA, RRP_{EQ}=17.4 nA, RRP_{decay}=16.8 nA and RRP_{NpRf}=17.8 nA). Note that the exponential fit to the data for the decay method (Fig. 4C, purple curve) is mostly hidden by the NpRf curve (black curve). For low p synapses, as in Fig. 4D where p_{NpRf}=0.10, the estimates of the methods diverged significantly. The model still provided a good fit to the data (Fig. 4D–F, *black line*), but now provided estimates of RRP that was intermediate between the train and EQ estimates (RRP_{train}= 5.9 nA, RRP_{EQ}=9.3 nA, RRP_{decay}=7.9 nA, and RRP_{NpRf}=8.5 nA). Looking at the data as a whole, we see that this observation represents a trend: RRP_{NpRf} is generally larger than RRP_{train} for almost all cases, and on average less than RRP_{EQ} (Fig. 5A and B). The deviations between RRP_{train} and RRP_{NpRf} were larger than deviations between RRP_{EQ} and RRP_{NpRf}, suggesting that the train method is poorly suited to estimate synaptic parameters when p is low. We compared RRP_{NpRf} to RRP_{decay}, which was calculated as $EPSC_0$ divided by p_{decay} (Fig. 5C). Results from the decay method tend to be close to those of the model, but diverge significantly for p<0.2. As expected, the reverse trends were observed when we compared p_{train}, p_{EQ}, and p_{decay} to p_{NpRf} (Fig. 5D–F), since for all three methods, the value of p is inversely related to the measure of RRP size. Note that estimates of p are all estimates of initial p: p_{train} and p_{EQ} are estimates of initial p, since they divide the amplitude of the first EPSC by the estimated RRP size, and p_{decay} and p_{NpRf} are corrected by facilitation factor f to reflect initial p.

The model appears to perform well even when p is low, as evidenced by very good agreement between the model fit to the data and the data itself even for p~0.1 (Fig. 4D–F). We reasoned that the model could improve our understanding of the conditions that lead the train and EQ methods to fail under certain conditions. We simulated synaptic responses according to our model by systematically varying one parameter while holding the others constant to observe how different methods of estimating RRP size perform. In these simulations, we held the facilitation parameter f equal to one, essentially excluding facilitation from our simulations. This was necessary because in many experiments (data not shown), the time course and magnitude of facilitation was very hard to measure at the calyx of Held, even under low Ca_e and pharmacological methods used in tandem to lower p. The extent of facilitation may therefore be more synapse-specific in a way that we cannot generally predict for simulation purposes. The effect of excluding facilitation from these simulations will be explored further in the Discussion.

First, we varied p while holding N_0 and R constant (Fig. 6A). We chose an RRP size equal to one for simplicity (N_0=1) and a replenishment rate (R=0.01), which is on the low end of the range of replenishment rates we observe in standard recording conditions. The ability of RRP_{train} to accurately estimate RRP size is highly dependent on the value of p; for high p, the RRP_{train} technique performed very well, with estimates of RRP size close to one (Fig. 6B, p=0.4 and 0.2), while its ability to accurately estimate RRP size is compromised at lower p values (Fig. 6B, p=0.1 and 0.05). When p=0.1, RRP_{train}=0.748, and when p=0.05, RRP_{train}=0.427. In contrast, the EQ method is affected much less by low p, in the absence of facilitation (Fig. 6C). In real data, we know that when p is low, facilitation begins to emerge. The difficulty of quantifying the average extent of facilitation as a function of p (discussed previously) prevented inclusion of facilitation into these simulations. These simulations can be summarized to show the relationship between RRP_{train} and RRP_{EQ} versus the true RRP size as dictated by the simulation (Fig. 6D). Our simulations suggest that RRP_{train} can be an

excellent estimate of RRP size for synapses with high p. They also reinforce that for low p synapses (i.e., for $p<0.4$), changes in p could be mistakenly attributed to changes in RRP size. This suggests that RRP_{train} can falsely report changes in p as changes in RRP for experimental manipulations, and should only be used under relatively high p conditions. They also show that the EQ method works very well in the absence of facilitation.

We then examined the effect of the rate of replenishment by systematically varying the replenishment rate, R, to determine how the replenishment rate affects estimates of RRP size (Fig. 7). The size of the RRP (N_0=1) and the probability of release (p=0.2) were held constant. If replenishment rates are very low, then the RRP_{train} and RRP_{EQ} techniques provide good assessments of true RRP size (Fig. 7A, B). For replenishment rates similar to what we observe at 100 Hz ($R \approx 0.02–0.04$), both methods deviate somewhat, and for higher rates of replenishment, estimates of RRP size become progressively worse. When R=0.1, RRP_{train}=0.53 and RRP_{EQ}=1.23. The systematic increase in the error associated with RRP_{train} and RRP_{EQ} as a function of R is summarized in Fig. 7C. Errors associated with the EQ method are smaller than those associated with the train method. These simulations highlight the sensitivity of the train and EQ methods to replenishment.

The frequency of stimulation has long been recognized as critical to reliable estimates of RRP size. It has been suggested that 300 Hz stimulus trains, but not 100 Hz stimulus trains, can deplete the RRP rapidly enough to ensure an accurate estimate of RRP size by the train method (Wu and Borst 1999; Sakaba 2006; Srinivasan et al. 2008), and it has been observed that 300 Hz stimulus trains analyzed with the RRP_{train} technique yield larger estimates of RRP size than 100 Hz stimulus trains (Taschenberger and von Gersdorff 2000). A study of the mouse neuromuscular junction used alternate methods to estimate RRP size, but similarly concluded that the true size of the RRP increases in size with stimulus frequency (Ruiz et al. 2011). It is not clear whether the higher frequency stimulation is required to obtain a more accurate measure of the size of a frequency-invariant RRP, or whether higher frequency stimulation is able to access a larger pool of vesicles. At other synapses, lower stimulus frequencies (20–40 Hz) are often used to estimate RRP_{train} (Wesseling and Lo 2002; Liu et al. 2014).

We decided to explore this issue at the calyx of Held using a modeling approach. We reasoned that the frequency of stimulation is closely related to the rate of replenishment with regard to the quantification of the RRP. To a first approximation, increasing the stimulus frequency is comparable to reducing the rate of replenishment, because in both cases there will be less replenishment between stimuli. We measured the time course of recovery from depression by 100 Hz stimulation, which could be fit with a double-exponential function (Fig. S1). This function was used to estimate the extent of recovery that would occur between stimuli for trains of frequencies faster and slower than 100 Hz (see Methods). We assessed the ability of the train and EQ methods to estimate RRP and p by performing simulations for a range of stimulus frequencies. Simulated EPSC amplitudes are plotted as a function of time (N_0=1; p=0.2; R=0.0295, the average replenishment rate for 100 Hz stimulation) (Fig. 8A) and as a function of stimulus number (Fig. 8B). The steady-state EPSC amplitude is much larger for lower-frequency stimulus trains than for fast stimulus trains because there is more replenishment between stimuli. For simulations in which only

stimulus frequency is changed, and not the RRP size, p, or replenishment rate per unit of time, there are substantial differences in the value of RRP_{train}, with low-frequency trains leading to considerable underestimates of RRP size (Fig. 8C). When the stimulus frequency is decreased, the assumption of constant replenishment throughout the train leads to larger errors. RRP_{EQ} estimates are also affected by stimulus frequency, with low-frequency trains leading to overestimates of RRP size (Fig. 8D). When the frequency is low and there is a great deal of replenishment between stimuli, it takes longer for the EPSC to reach steady-state amplitude.

We also examined how R and p interact with frequency to influence the estimates of RRP size with the EQ and train methods. Summary plots of estimated RRP size versus stimulus frequency are shown for a fixed rate of replenishment ($R=R_{avg}=0.0295$) for different p (Fig. 8E*;* p=0.1, 0.2, 0.4). For all conditions, higher stimulus frequencies provide better estimates of the RRP size, although each preparation has practical limitations on how rapidly presynaptic axons can be reliably stimulated (see Discussion). Changing p has a large influence on RRP_{train}. For 100 Hz stimulation, p=0.4 yields RRP_{train}=0.920, p=0.2 yields RRP_{train}=0.803 and p=0.1 yields RRP_{train}=0.591, even though in all cases the N_0 was set equal to one. When p is below 0.2, there are considerable errors in estimating the RRP with the train method. Interestingly, when R is fixed, the RRP_{EQ} technique is highly resistant to changes in p in our simulated data (Fig. 8E, blue lines overlap for p=0.1, 0.2 and 0.4). As a result, the performance of the EQ method is much better than the train method when p is less than 0.2.

We also assessed the role of changing stimulus frequency under conditions of reduced or enhanced replenishment of the RRP for p=0.2 (Fig. 8F, $R=0.5R_{avg}$, R_{avg}, and $2R_{avg}$). We find that both the train and EQ methods are sensitive to changes in replenishment, as would be expected from the results shown in Fig. 7. At 100 Hz, doubling the replenishment rate reduces RRP_{train} considerably (R_{avg}: RRP_{train}=0.803, red curve; $2R_{avg}$: RRP_{train}=0.667, light red curve). Halving the replenishment rate improves the ability of the RRP_{train} method to accurately assess RRP size ($0.5R_{avg}$: RRP_{train}=0.890, dark red curve). Doubling the replenishment rate increases RRP_{EQ} (R_{avg}: RRP_{EQ}=1.061, blue curve; $2R_{avg}$: RRP_{EQ}=1.126, light blue curve), and halving it improves the RRP_{EQ} estimate of RRP size ($0.5R_{avg}$: RRP_{train}=1.030, dark blue curve).

The summaries in Fig. 8E–F indicate how stimulus frequency, the probability of release, and replenishment can together influence the performance of the EQ and train methods. The train method, which is the most widely used method to quantify RRP, significantly underestimates RRP when p is low, when replenishment is rapid, and when the stimulus frequency is low. The performance of the EQ method is in general superior to the train method in that it is less sensitive to changes in p, but considerably overestimates RRP when the frequency is low and replenishment is high. Additionally, the presence of substantial facilitation, as at other synapses or at very low p conditions at the calyx of Held, will also compromise EQ estimates.

In light of these simulations, we analyzed experimental data collected at 100 Hz and 200 Hz with our four techniques. Here, we show an example cell with the train technique applied,

and see that the estimate of RRP is larger for 200 Hz stimulation than it is for 100 Hz stimulation (Fig. 9A). This could either reflect an increase in the number of vesicles that are readily released when the stimulus frequency is elevated, or it could reflect a problem with the estimate of the RRP that is suggested by the simulations of Fig. 8. We also used the EQ method, the decay method and the NpRf model to estimate RRP size at 100 Hz and 200 Hz (Figs. 9B–D) and found only small differences in estimates of RRP size and p at the different stimulus frequencies. Our summary data (Fig. 9E) shows that the train method reports differences in RRP size, and consequently, differences in p, for different stimulus frequencies. In contrast, the EQ method, decay method, and NpRf model all report more similar values for RRP size and p at 100 Hz and 200 Hz, with the NpRf and decay methods reporting the least difference. These experimental results align with the predictions of the simulations in Fig. 8, and suggest that the use of multiple approaches to analyze responses evoked by trains provides a more robust means of estimating synaptic parameters.

4. Discussion

4.1 Assessment of the NpRf model in comparison to three other methods

Our goal was to determine the best way to accurately measure the size of the RRP and p using stimulus trains. We characterized four independent methods at the calyx of Held synapse and find that for $p>0.4$, all exhibit remarkable agreement, providing confidence in the values we obtain. The estimates began to diverge for $p<0.4$, warranting further analysis of these methods. We began by investigating the train and EQ methods, which are the most widely used methods used to analyze action potential evoked release at high p synapses. A comparison of postsynaptic responses from individual cells shows that RRP_{EQ} is consistently greater than RRP_{train} when $p<0.4$ (Fig. 2). Our simulations suggest that this is a consequence of the different assumptions each method makes regarding replenishment. While the EQ method does not subtract any release of newly-replenished vesicles from its estimation of RRP size, the train method subtracts a maximal level of replenishment. This would lead to a systematic overestimation of RRP size by the EQ method and underestimation by the train method, which is consistent with our results.

To deepen our understanding of synaptic parameters at the calyx of Held, we also applied the decay method to directly estimate p. The observation that single-exponential functions fit our data very well (Fig. 3C) suggests that a 100 Hz train of action potentials primarily liberates a pool of vesicles that have approximately the same p. Although previous studies found that prolonged voltage steps liberated two components of release at the calyx of Held (Sakaba and Neher 2001a, 2001b; Wölfel et al. 2007; Schneggenburger et al. 2012), recent work suggests that a single fast pool is likely responsible for action potential-evoked release (Chen et al. 2015). The decay method yields excellent agreement with both the train and EQ methods for $p>0.4$, and this can be extended by correcting for facilitation to extend its range. However, for $p<0.2$, p_{decay} tends to be lower than p_{train} and considerably greater than p_{EQ} (Fig. 3G, H), and the decay method estimates diverge from train and EQ estimates even more substantially at very low p (Fig. 3I, J).

Encouraged by the results of the decay method, we developed and applied a simple model that implements depletion of the RRP with a more accurate description of replenishment in

which refilling of the RRP proceeds with a constant rate per available release site. The number of available release sites increases during the beginning of an action potential train as the RRP is depleted, and eventually stabilizes at a steady-state value. We deliberately kept the model very simple, which was possible for our goal of studying synchronous, evoked release of neurotransmitter in response to a regular, high-frequency train stimuli. We kept the number of parameters small and did not incorporate physical models of the presynaptic machinery (Meinrenken et al. 2002; Pan and Zucker 2009) that require many parameters to account for active zone size, the location and density of calcium channels, the concentration and binding properties of calcium buffers, as well as parameters to describe vesicle pools with different properties and calcium-dependent recovery from depression (Dittman and Regehr 1998; Dittman et al. 2000; Yang and Xu-Friedman 2008; Hallermann et al. 2010).

We found that the NpRf model very cleanly fit the data we have collected in a variety of pharmacological and external calcium conditions (Figs. 4 and 5). RRP_{NpRf}, RRP_{train}, RRP_{EQ}, and RRP_{decay} are all in agreement when p is high, but when p is low RRP_{NpRf} is typically greater than RRP_{train} and RRP_{decay} but less than RRP_{EQ} (Fig. 5). This is consistent with the prediction that the different methods' corrections for replenishment will lead RRP_{train} to underestimate RRP and RRP_{EQ} to overestimate it, and suggests that RRP_{NpRf} can provide a more reliable means of estimating RRP and p. RRP_{NpRf} also differs from RRP_{decay}, especially for low p, suggesting that accounting for a variable rate of replenishment significantly affects the NpRf method's estimates of p and RRP size.

It is also possible that in addition to the component of release described by the train methods, there could also be a component of release with a much lower p (Müller et al. 2010). Such a component of release may not play a large role in determining the rapid responses to the onset of a train stimulus, but could be important for sustaining release during prolonged high frequency stimulation that can occur under physiological conditions. It is likely that other methods to determine the size of the RRP, such as using large voltage steps or high osmolarity (Schneggenburger et al. 2002; Zucker and Regehr 2002; Schneggenburger and Neher 2005), liberate pools of vesicles that do not make substantial contributions to release evoked by high frequency stimulation. Different pools of vesicles evoked by large voltage steps have been identified, but it has been difficult to relate such pools to different aspects of action potential evoked release. Using high osmolarity and large voltage step methods does not discriminate between high p and low p components of release; instead, they simply compute average p. These methods may even liberate vesicles that cannot be liberated by action potentials. This may provide an incomplete view of release. For example, a neuromodulator could increase the size of the high p pool by transforming low p sites into high p sites. Train methods would detect an increase in RRP and no change in p, but step and high osmolarity measurements would detect no change in RRP and would conclude that p increased. This points out potential challenges in relating estimates of p and RRP size based on different approaches and highlights the difficulty in defining the RRP.

4.2 Step by step approach to determine synaptic parameters using stimulus trains

The approach we took to evaluate the performance of EQ and train methods is a best-case scenario at a close-to-ideal high-*p* synapse, the calyx of Held. There are many challenges that can further affect the performance of these methods at other synapses. It is useful to explicitly consider the complications that can be encountered and the general steps that must be taken to best estimate *p* and RRP from the amplitudes of synaptic currents evoked by trains.

Determine whether the synapse is a depressing or facilitating—Train methods only give reliable estimates for depressing synapses or synapses with modest facilitation. For facilitating synapses with a low initial probability of release other approaches must be used (see below).

Determine if postsynaptic saturation or desensitization of postsynaptic receptors influences short-term plasticity—Such postsynaptic factors make synaptic currents inaccurate measures of neurotransmitter release. For glutamatergic synapses, low-affinity AMPA receptor antagonists such as kynurenic acid and γDGG are used to relieve saturation (Watkins et al. 1990; Liu et al. 1999; Wadiche and Jahr 2001) and cyclothiazide is used to relieve desensitization (Trussell et al. 1993; Otis et al. 1996; Neher and Sakaba 2001). Typically, if these drugs alter short-term plasticity, then synaptic parameters must be characterized in their presence to avoid saturation or desensitization. We used kynurenic acid and cyclothiazide at concentrations previously shown to prevent receptor saturation and desensitization at the calyx of Held synapse (Neher and Sakaba 2001). At inhibitory synapses, the low-affinity antagonist TPMPA can be used to relieve receptor saturation of $GABA_A$ receptors (Jones et al. 2001; Sakaba 2008), but for many types of receptors, low-affinity antagonists may not be available. Synaptic parameters must be determined under conditions where the contributions of saturation and desensitization are eliminated.

Determine if presynaptic axons be activated at sufficiently high frequency relative to the replenishment rate—Our simulations indicate that it is possible to more reliably estimate synaptic parameters when the firing frequency is fast relative to the rate of replenishment (Figs. 7 and 8). For the train method, recent modeling suggests that postsynaptic responses must depress by at least 60% to obtain reliable estimate synaptic parameters (Neher 2015). Our simulations and experimental findings suggest that the performance of train methods can be substantially degraded even when the steady-state responses are depressed by 80% (Fig. 7). There is a limit to how rapidly presynaptic fibers can be reliably activated. For the calyx of Held, which fires at least up to 300 Hz in adult mice (Borst and Soria van Hoeve 2012), the capacity of presynaptic axons to fire in slice experiments is highly age- and temperature- dependent. In our experience, calyces of Held in tissue from mice aged P11-14 can be reliably stimulated at frequencies up to 100–200 Hz at 25°C, and at 300 Hz or higher at 34°C. It may be possible to stimulate even more rapidly in older animals at high temperature. It is important to realize that performing experiments at high temperature in older animals to allow more rapid stimulation may not provide a better estimate of pool size, because replenishment may be more rapid at physiological temperature in older animals.

Accurately measure the amplitude of synaptic currents in response to high-frequency stimulation—For a given data set, individual recordings must be evaluated to ensure that automatic quantification of postsynaptic current amplitudes (PSC) is being performed accurately. Slight inaccuracies can obscure the actual dynamics of RRP depletion and recovery. The baseline current must be subtracted from the peak of the PSC. Moreover, if PSCs decay slowly, such that the decay is longer than the interstimulus interval of the stimulus train, this must be accounted for in quantifying PSC amplitude. A single or double exponential fit to the decay of the previous PSC should be obtained and subtracted from the following PSC in order to measure its amplitude.

Determine if EPSC amplitudes during high-frequency trains are primarily determined by depletion of a single pool of vesicles with a uniform probability of release—The EQ method, the decay method, and the NpRf method all rely on p remaining constant throughout a stimulus train after an initial facilitation and on depletion dominating the decrement of synaptic responses during the train. The train method does not require constant p, but does require depletion of the RRP by rapid stimulation. Although depletion of the RRP accounts for depression at many synapses, this is not the case for all synapses. Also, for many low p synapses, p increases during stimulus trains as a result of synaptic facilitation, which will pose problems in the measurement of RRP. The EQ method, the decay method and the NpRf method all require release to be mediated by a single pool of vesicles with uniform p. There is considerable evidence that release sites from the same presynaptic active zone can have different probabilities of release. At the calyx of Held, numerous studies have reported the existence of a fast-releasing pool (FRP) and slow-releasing pool (SRP) which are elicited by presynaptic voltage steps and presynaptic caged calcium experiments (Sakaba and Neher 2001a; Wölfel et al. 2007). We found that despite evidence that there are different pools of vesicles with different properties when release is evoked by non-AP stimuli, there was not a clear indication of a fast and slow component to the pool of vesicles released by high-frequency APs. This contrasts with studies performed at this synapse at lower frequencies (Trommershäuser et al. 2003). Plots of the EPSC amplitude as a function of stimulus number (as in Fig. 3C) could be fit well with a single exponential function, indicating that release is dominated by a pool of vesicles with an approximately uniform p. This cannot rule out the possibility that there is a contribution of a second, slower pool to AP-evoked release, as suggested by others, but does give us confidence that a slower pool does not make a large contribution under the experimental conditions applied here. This is a very important point for researchers who may apply these techniques to a given synapse--if AP-evoked release appears to be driven by multiple vesicle pools with different release probabilities, then the EQ and decay methods would give erroneous estimates of synaptic parameters that would differ considerably from estimates based on the train method. It is expected that the train and EQ methods will determine the size of the RRP and probability of release, and are likely to significantly underestimate the true size of the RRP if there are multiple pools or heterogeneous release probabilities.

Determine if responses reach a true steady state after prolonged stimulation —The train method relies on release reaching a steady-state value, and if this is not the case it will not provide a reliable estimate of RRP size. We have found that this is the case at the

calyx of Held synapse on the relatively short time scale of our experiments. This is not always the case at other synapses. One factor that could prevent the attainment of a steady state would be if stimulation began to deplete the reserve pool, which would in turn reduce replenishment of the RRP during sustained activation. It is also possible that a pool with a very low probability of release would only very gradually deplete and prevent steady state from being attained. If the EPSC amplitude does not stabilize at a steady value, then it is not possible to apply the train method to determine the size of the RRP.

Compare the estimates of the 4 different methods—If the conditions of the different methods are not satisfied then they cannot be applied. A comparison of the different methods that can be applied provides a powerful means to evaluate the various estimates because they are based on different assumptions. Good agreement between the different methods, as is predicted to be the case when the initial p is high, will validate the estimates. If p is moderate to low then disagreements between the methods are expected, but the differences should conform to the predictions of the simulations present here and the *NpRf* model should provide a good estimate. This comprehensive approach will provide insight into the synapse and will extract as much information as possible from responses evoked by stimulus trains.

4.4 Stochastic variability and estimates of synaptic parameters

Stochastic variability in synaptic strength differentially influences the ability of each method to estimate synaptic parameters. For example, the EQ method, which is based on a linear fit to just four data points, seems to be particularly sensitive to stochastic variability. It is also possible that noise could systematically bias estimates of synaptic parameters and contribute to the differences in estimates of synaptic strength made with different approaches. For the large calyx of Held synapses we study, it appears that estimates of different methods conform to predictions based on models of synaptic strength. However, variability in synaptic responses become increasingly important for smaller synapses consisting of fewer release sites and the train methods described here become ineffective. Approaches based on quantal analysis, such as variance-mean analysis and multiple probability fluctuation analysis (MPFA) provide a powerful alternative approach that can be used to characterize low p synapses or synapses with few release sites (Redman 1990; Bekkers 1994; Silver et al. 1998; Reid and Clements 1999; Bennett and Kearns 2000; Meyer et al. 2001; Neher and Sakaba 2001; Silver 2003; Foster and Regehr 2004). These methods require low-frequency repetitive activation of synapses and use fluctuations in the amplitudes of the resulting postsynaptic responses to determine N_0, p, and q. These quantal approaches are challenging to apply because they require many trials from at least three different release probability conditions (typically different external calcium concentrations) and very stable, high signal-to-noise recordings. Moreover, pharmacological agents must be used to eliminate postsynaptic receptor saturation and desensitization to accurately estimate synaptic parameters. Nonetheless, quantal approaches may be the methods of choice for estimating synaptic parameters at non-depressing or facilitating synapses. These are likely preferable to using a high-frequency approach with artificially elevated Ca_e to increase p and deplete the RRP. Substantial elevation of external calcium may trigger non-physiological vesicular

release, primarily due to artificial temporal and spatial enlargement of calcium nano- or micro-domains at the active zone.

We hope that this analysis of existing methods and the presentation of a simple model (NpRf method) at the calyx of Held can be useful to investigators when considering the best way to estimate the values of synaptic parameters such as N_0, p, and R. These methods may also be applicable to other depressing synapses with prominent depletion, such as the endbulb of Held and neuromuscular junction (Elmqvist and Quastel 1965; Yang and Xu-Friedman 2008).

The choice of methods to analyze data from a given synapse can have important implications for our ability to understand synaptic transmission. As shown by simulations in Figs. 6–8, using the train or EQ method below $p<0.2$ under our conditions can lead to changes in p, R, or firing frequency as being inaccurately attributed to changes in N_0. For the train and EQ methods, incorrect estimates of RRP size will have a direct consequence of making estimates of p inaccurate as well. This is much more important than an issue of semantics—different molecules and plasticity regimes regulate various aspects of synaptic transmission, and in many cases should only change N_0 or p. If investigators use appropriate methods to analyze genetic mutants, pharmacological agents, or plasticity regimes, the findings can direct follow-up studies to characterize the mechanism or locus of action.

Supplementary Material

Refer to Web version on PubMed Central for supplementary material.

Acknowledgments

We thank members of the Regehr laboratory for their comments on this manuscript. This work was supported by NIH grant NS032405 to WGR and NIH grant F31 NS073252 to MST.

References

Abbott ALF, Varela JA, Sen K, Nelson SB. Synaptic Depression and Cortical Gain Control. Science. 1997; 275(5297):220–4. [PubMed: 8985017]

Bekkers JM. Quantal analysis of synaptic transmission in the central nervous system. Curr Opin Neurobiol [Internet]. 1994 Jun; 4(3):360–5. cited 2016 Jan 29. Available from: http://www.ncbi.nlm.nih.gov/pubmed/7919931.

Bennett MR, Kearns JL. Statistics of transmitter release at nerve terminals. Prog Neurobiol [Internet]. 2000 Apr; 60(6):545–606. cited 2016 Feb 2. Available from: http://www.sciencedirect.com/science/article/pii/S0301008299000404.

Borst JGG, Soria van Hoeve J. The calyx of held synapse: from model synapse to auditory relay. Annu Rev Physiol [Internet]. 2012 Jan.74:199–224. cited 2014 Mar 21. Available from: http://www.ncbi.nlm.nih.gov/pubmed/22035348.

Cartling B. Control of neural information transmission by synaptic dynamics. J Theor Biol [Internet]. 2002 Jan 21; 214(2):275–92. cited 2014 Jan 21. Available from: http://www.ncbi.nlm.nih.gov/pubmed/11812178.

Chen Z, Das B, Nakamura Y, DiGregorio DA, Young SM. Ca2+ channel to synaptic vesicle distance accounts for the readily releasable pool kinetics at a functionally mature auditory synapse. J Neurosci [Internet]. 2015 Feb 4; 35(5):2083–100. cited 2015 Feb 10. Available from: http://www.jneurosci.org/content/35/5/2083.short.

Dittman JS, Kreitzer AC, Regehr WG. Interplay between facilitation, depression, and residual calcium at three presynaptic terminals. J Neurosci [Internet]. 2000 Feb 15; 20(4):1374–85. Available from: http://www.ncbi.nlm.nih.gov/pubmed/10662828.

Dittman JS, Regehr WG. Calcium dependence and recovery kinetics of presynaptic depression at the climbing fiber to Purkinje cell synapse. J Neurosci [Internet]. 1998 Aug 15; 18(16):6147–62. Available from: http://www.ncbi.nlm.nih.gov/pubmed/9698309.

Dobrunz LE, Stevens CF. Heterogeneity of release probability, facilitation, and depletion at central synapses. Neuron [Internet]. 1997 Jun; 18(6):995–1008. Available from: http://www.ncbi.nlm.nih.gov/pubmed/9208866.

Elmqvist BYD, Quastel DMJ. A quantitave study of end-plate potentials in isolated human muscle. J Physiol. 1965; 178:505–29. [PubMed: 5827910]

Fioravante, D.; Chu, Y.; Myoga, MH.; Leitges, M.; Regehr, WG. Neuron [Internet]. Vol. 70. Elsevier Inc; 2011 Jun 9. Calcium-dependent isoforms of protein kinase C mediate posttetanic potentiation at the calyx of Held; p. 1005-19.cited 2013 Sep 26Available from: http://www.pubmedcentral.nih.gov/articlerender.fcgi?artid=3113702&tool=pmcentrez&rendertype=abstract

Foster KA, Regehr WG. Variance-mean analysis in the presence of a rapid antagonist indicates vesicle depletion underlies depression at the climbing fiber synapse. Neuron [Internet]. 2004 Jul 8; 43(1): 119–31. cited 2014 Aug 13. Available from: http://www.sciencedirect.com/science/article/pii/S0896627304003903.

Gaviño MA, Ford KJ, Archila S, Davis GW. Homeostatic synaptic depression is achieved through a regulated decrease in presynaptic calcium channel abundance. Elife [Internet]. 2015 Apr 17.4 cited 2015 Apr 20. Available from: http://www.pubmedcentral.nih.gov/articlerender.fcgi?artid=4443758&tool=pmcentrez&rendertype=abstract.

Hallermann S, Heckmann M, Kittel RJ. Mechanisms of short-term plasticity at neuromuscular active zones of Drosophila. HFSP J. 2010; 4(2):72–84. [PubMed: 20811513]

Hennig MH. Theoretical models of synaptic short term plasticity. Front Comput Neurosci [Internet]. 2013; 7(April):45. Available from: http://www.pubmedcentral.nih.gov/articlerender.fcgi?artid=3630333&tool=pmcentrez&rendertype=abstract.

Hosoi N, Sakaba T, Neher E. Quantitative analysis of calcium-dependent vesicle recruitment and its functional role at the calyx of Held synapse. J Neurosci [Internet]. 2007 Dec 26; 27(52):14286–98. cited 2014 Feb 5. Available from: http://www.ncbi.nlm.nih.gov/pubmed/18160636.

Iwasaki S, Takahashi T. Rapid Report Developmental changes in calcium channel types mediating synaptic transmission in rat auditory brainstem. J Physiol. 1998; 509(2):419–23. [PubMed: 9575291]

Jones MV, Jonas P, Sahara Y, Westbrook GL. Microscopic kinetics and energetics distinguish GABA(A) receptor agonists from antagonists. Biophys J [Internet] Elsevier. 2001; 81(5):2660–70. Available from: http://dx.doi.org/10.1016/S0006-3495(01)75909-7.

Kusano K, Landau EM. Depression and recovery of transmission at the squid giant synapse. J Physiol [Internet]. 1975 Feb; 245(1):13–32. cited 2014 Apr 1. Available from: http://www.pubmedcentral.nih.gov/articlerender.fcgi?artid=1330842&tool=pmcentrez&rendertype=abstract.

Liley AW, North KAK. An electrical investigation of effects of repetitive stimulation on mammalian neuromuscular junction. J Neurophysiol [Internet]. 1953 Sep 1; 16(5):509–27. cited 2014 Mar 12. Available from: http://jn.physiology.org.ezp-prod1.hul.harvard.edu/content/16/5/509.

Liu G, Choi S, Tsien RW. Variability of neurotransmitter concentration and nonsaturation of postsynaptic AMPA receptors at synapses in hippocampal cultures and slices. Neuron. 1999; 22(2):395–409. [PubMed: 10069344]

Liu, H.; Bai, H.; Hui, E.; Yang, L.; Evans, CS.; Wang, Z., et al. Elife [Internet]. Vol. 3. eLife Sciences Publications, Ltd; 2014 Jan. Synaptotagmin 7 functions as a Ca2+-sensor for synaptic vesicle replenishment; p. e01524cited 2014 Mar 26Available from: /pmc/articles/PMC3930910/?report=abstract

Meinrenken CJ, Borst JGG, Sakmann B. Calcium secretion coupling at calyx of held governed by nonuniform channel-vesicle topography. J Neurosci [Internet]. 2002 Mar 1; 22(5):1648–67. Available from: http://www.ncbi.nlm.nih.gov/pubmed/11880495.

Meyer AC, Neher E, Schneggenburger R. Estimation of Quantal Size and Number of Functional Active Zones at the Calyx of Held Synapse by Nonstationary EPSC Variance Analysis. J Neurosci [Internet]. 2001 Oct 15; 21(20):7889–900. cited 2016 Jan 29. Available from: http://www.jneurosci.org.ezp-prod1.hul.harvard.edu/content/21/20/7889.long.

Moulder KL, Mennerick S. Reluctant vesicles contribute to the total readily releasable pool in glutamatergic hippocampal neurons. J Neurosci [Internet]. 2005 Apr 13; 25(15):3842–50. cited 2013 Nov 15. Available from: http://www.ncbi.nlm.nih.gov/pubmed/15829636.

Müller M, Genç Ö, Davis GW. RIM-Binding Protein Links Synaptic Homeostasis to the Stabilization and Replenishment of High Release Probability Vesicles. Neuron [Internet]. 2015 Feb 4; 85(5): 1056–69. cited 2015 Feb 23. Available from: http://www.ncbi.nlm.nih.gov/pubmed/25704950.

Müller M, Goutman JD, Kochubey O, Schneggenburger R. Interaction between facilitation and depression at a large CNS synapse reveals mechanisms of short-term plasticity. J Neurosci. 2010; 30(6):2007–16. [PubMed: 20147529]

Neher E. Merits and Limitations of Vesicle Pool Models in View of Heterogeneous Populations of Synaptic Vesicles. Neuron [Internet]. 2015 Sep 23; 87(6):1131–42. cited 2015 Sep 28. Available from: http://www.sciencedirect.com/science/article/pii/S0896627315007564.

Neher E, Sakaba T. Combining deconvolution and noise analysis for the estimation of transmitter release rates at the calyx of held. J Neurosci [Internet]. 2001 Jan 15; 21(2):444–61. Available from: http://www.ncbi.nlm.nih.gov/pubmed/11160425.

Neher E, Sakaba T. Multiple roles of calcium ions in the regulation of neurotransmitter release. Neuron [Internet]. 2008 Sep 25; 59(6):861–72. cited 2015 Jun 17. Available from: http://www.sciencedirect.com/science/article/pii/S0896627308007423.

Otis T, Zhang S, Trussell LO. Direct Measurement of AMPA Receptor Desensitization Induced by Glutamatergic Synaptic Transmission. J Neurosci [Internet]. 1996 Dec 1; 16(23):7496–504. cited 2016 Feb 16. Available from: http://www.jneurosci.org.ezp-prod1.hul.harvard.edu/content/16/23/7496.long.

Pan B, Zucker RS. A General Model of Synaptic Transmission and Short-Term Plasticity. Neuron [Internet] Elsevier Ltd. 2009; 62(4):539–54. Available from: http://dx.doi.org/10.1016/j.neuron.2009.03.025.

Redman S. Quantal analysis of synaptic potentials in neurons of the central nervous system. Physiol Rev [Internet]. 1990 Jan; 70(1):165–98. cited 2016 Feb 2. Available from: http://www.ncbi.nlm.nih.gov/pubmed/2404288.

Reid CA, Clements JD. Postsynaptic expression of long-term potentiation in the rat dentate gyrus demonstrated by variance-mean analysis. J Physiol [Internet]. 1999 Jul 8; 518(1):121–30. cited 2016 Jan 29. Available from: http://doi.wiley.com/10.1111/j.1469-7793.1999.0121r.x.

Ruiz R, Cano R, Casañas JJ, Gaffield MA, Betz WJ, Tabares L. Active zones and the readily releasable pool of synaptic vesicles at the neuromuscular junction of the mouse. J Neurosci [Internet]. 2011 Feb 9; 31(6):2000–8. cited 2015 Jul 19. Available from: http://www.jneurosci.org.ezp-prod1.hul.harvard.edu/content/31/6/2000.long.

Sakaba T. Roles of the fast-releasing and the slowly releasing vesicles in synaptic transmission at the calyx of Held. J Neurosci [Internet]. 2006 May 31; 26(22):5863–71. cited 2015 Jul 22. Available from: http://www.jneurosci.org.ezp-prod1.hul.harvard.edu/content/26/22/5863.long.

Sakaba T. Two Ca2+-Dependent Steps Controlling Synaptic Vesicle Fusion and Replenishment at the Cerebellar Basket??Cell Terminal. Neuron. 2008; 57(3):406–19. [PubMed: 18255033]

Sakaba T, Neher E. Calmodulin mediates rapid recruitment of fast-releasing synaptic vesicles at a calyx-type synapse. Neuron [Internet]. 2001a Dec 20; 32(6):1119–31. Available from: http://www.ncbi.nlm.nih.gov/pubmed/11754842.

Sakaba T, Neher E. Quantitative relationship between transmitter release and calcium current at the calyx of held synapse. J Neurosci [Internet]. 2001b Jan 15; 21(2):462–76. Available from: http://www.ncbi.nlm.nih.gov/pubmed/11160426.

Schneggenburger R, Han Y, Kochubey O. Ca(2+) channels and transmitter release at the active zone. Cell Calcium [Internet]. 2012 Jan; 52(3–4):199–207. cited 2014 Feb 18. Available from: http://www.sciencedirect.com/science/article/pii/S0143416012000814.

Schneggenburger R, Meyer aC, Neher E. Released fraction and total size of a pool of immediately available transmitter quanta at a calyx synapse. Neuron [Internet]. 1999 Jun; 23(2):399–409. Available from: http://www.ncbi.nlm.nih.gov/pubmed/10399944.

Schneggenburger R, Neher E. Presynaptic calcium and control of vesicle fusion. Curr Opin Neurobiol [Internet]. 2005 Jun; 15(3):266–74. cited 2013 Sep 16. Available from: http://www.ncbi.nlm.nih.gov/pubmed/15919191.

Schneggenburger R, Sakaba T, Neher E. Vesicle pools and short-term synaptic depression: lessons from a large synapse. Trends Neurosci [Internet]. 2002 Apr; 25(4):206–12. Available from: http://www.ncbi.nlm.nih.gov/pubmed/11998689.

Schneider T, Wei X, Olcese R, Costantin J, Neely A, Palade P, et al. Molecular analysis and functional expression of the human type E neuronal Ca2+ channel alpha 1 subunit. Recept Channels. 1994; 2(4):255–70. [PubMed: 7536609]

Silver RA. Estimation of nonuniform quantal parameters with multiple-probability fluctuation analysis: theory, application and limitations. J Neurosci Methods [Internet]. 2003 Dec; 130(2): 127–41. cited 2016 Jan 27. Available from: http://www.sciencedirect.com/science/article/pii/S0165027003003170.

Silver RA, Momiyama A, Cull-Candy SG. Locus of frequency-dependent depression identified with multiple-probability fluctuation analysis at rat climbing fibre-Purkinje cell synapses. J Physiol [Internet]. 1998 Aug 22; 510(3):881–902. cited 2016 Jan 27. Available from: http://doi.wiley.com/10.1111/j.1469-7793.1998.881bj.x.

Soong TW, Stea A, Hodson CD, SJD, Vincent SR, Snutch TP. Structure and functional expression of a member of the low voltage-activated calcium channel family. Science (80-). 1993; 260:1133–6.

Srinivasan G, Kim JH, von Gersdorff H. The pool of fast releasing vesicles is augmented by myosin light chain kinase inhibition at the calyx of Held synapse. J Neurophysiol [Internet]. 2008 Apr 1; 99(4):1810–24. cited 2015 Jul 22. Available from: http://jn.physiology.org.ezp-prod1.hul.harvard.edu/content/99/4/1810.long.

Stevens CF, Williams JH. Discharge of the readily releasable pool with action potentials at hippocampal synapses. J Neurophysiol [Internet]. 2007 Dec; 98(6):3221–9. cited 2014 Apr 5. Available from: http://www.pubmedcentral.nih.gov/articlerender.fcgi?artid=2201901&tool=pmcentrez&rendertype=abstract.

Takahashi T, Kajikawa Y, Tsujimoto T. G-Protein-Coupled Modulation of Presynaptic Calcium Currents and Transmitter Release by a GABA B Receptor. 1998; 18(9):3138–46.

Taschenberger H, von Gersdorff H. Fine-tuning an auditory synapse for speed and fidelity: developmental changes in presynaptic waveform, EPSC kinetics, and synaptic plasticity. J Neurosci [Internet]. 2000 Dec 15; 20(24):9162–73. Available from: http://www.ncbi.nlm.nih.gov/pubmed/11124994.

Thanawala MS, Regehr WG. Presynaptic calcium influx controls neurotransmitter release in part by regulating the effective size of the readily releasable pool. J Neurosci [Internet]. 2013 Mar 13; 33(11):4625–33. cited 2014 May 26. Available from: http://www.pubmedcentral.nih.gov/articlerender.fcgi?artid=3711668&tool=pmcentrez&rendertype=abstract.

Trommershäuser J, Schneggenburger R, Zippelius A, Neher E. Heterogeneous presynaptic release probabilities: functional relevance for short-term plasticity. Biophys J [Internet]. 2003 Mar; 84(3): 1563–79. cited 2014 Feb 6. Available from: http://www.sciencedirect.com/science/article/pii/S0006349503749674.

Trussell LO, Zhang S, Ramant IM. Desensitization of AMPA receptors upon multiquantal neurotransmitter release. Neuron [Internet]. 1993 Jun; 10(6):1185–96. cited 2016 Feb 16. Available from: http://www.sciencedirect.com/science/article/pii/089662739390066Z.

Tsodyks MV, Markram H. The neural code between neocortical pyramidal neurons depends on neurotransmitter release probability. Proc Natl Acad Sci U S A [Internet]. 1997 Jan 21; 94(2):719–23. cited 2014 Apr 5. Available from: http://www.pubmedcentral.nih.gov/articlerender.fcgi?artid=19580&tool=pmcentrez&rendertype=abstract.

Wadiche JI, Jahr CE. Multivesicular Release at Climbing Fiber-Purkinje Cell Synapses. Neuron [Internet]. 2001 Oct; 32(2):301–13. cited 2014 Aug 13. Available from: http://www.sciencedirect.com/science/article/pii/S0896627301004883.

Wang LY, Kaczmarek LK. High-frequency firing helps replenish the readily releasable pool of synaptic vesicles. Nature [Internet]. 1998 Jul 23; 394(6691):384–8. Available from: http://www.ncbi.nlm.nih.gov/pubmed/9690475.

Watkins JC, Pook PC, Sunter DC, Davies J, Honore T. Experiments with kainate and quisqualate agonists and antagonists in relation to the sub-classification of “non-NMDA” receptors. Adv Exp Med Biol [Internet]. 1990 Jan.268:49–55. cited 2016 Jan 22. Available from: http://www.ncbi.nlm.nih.gov/pubmed/1963751.

Wesseling JF, Lo DC. Limit on the role of activity in controlling the release-ready supply of synaptic vesicles. J Neurosci [Internet]. 2002 Nov 15; 22(22):9708–20. Available from: http://www.ncbi.nlm.nih.gov/pubmed/12427826.

Wölfel M, Lou X, Schneggenburger R. A mechanism intrinsic to the vesicle fusion machinery determines fast and slow transmitter release at a large CNS synapse. J Neurosci [Internet]. 2007 Mar 21; 27(12):3198–210. cited 2014 Feb 12. Available from: http://www.ncbi.nlm.nih.gov/pubmed/17376981.

Wu L-G, Borst JGG. The Reduced Release Probability of Releasable Vesicles during Recovery from Short-Term Synaptic Depression. Neuron [Internet]. 1999 Aug; 23(4):821–32. cited 2014 Apr 1. Available from: http://www.sciencedirect.com/science/article/pii/S0896627301800398.

Wu LG, Borst JGG, Sakmann B. R-type Ca2+ currents evoke transmitter release at a rat. J Neurosci. 1998; 95(April):4720–5.

Wu LG, Westenbroek RE, Borst JGG, Catterall WA, Sakmann B. Calcium channel types with distinct presynaptic localization couple differentially to transmitter release in single calyx-type synapses. J Neurosci [Internet]. 1999 Jan 15; 19(2):726–36. Available from: http://www.ncbi.nlm.nih.gov/pubmed/9880593.

Yang H, Xu-Friedman Ma. Relative roles of different mechanisms of depression at the mouse endbulb of Held. J Neurophysiol. 2008; 99(5):2510–21. [PubMed: 18367696]

Zamponi GW, Bourinet E, Snutch TP. Nickel Block of a Family of Neuronal Calcium Channels: Subtype- and Subunit-Dependent Action at Multiple Sites. J Membr Biol [Internet]. 1996 May 1; 151(1):77–90. Available from: http://link.springer.com/10.1007/s002329900059.

Zucker RS, Regehr WG. Short-term synaptic plasticity. Annu Rev Physiol [Internet]. 2002 Jan.64:355–405. cited 2014 Jan 21. Available from: http://www.ncbi.nlm.nih.gov/pubmed/11826273.

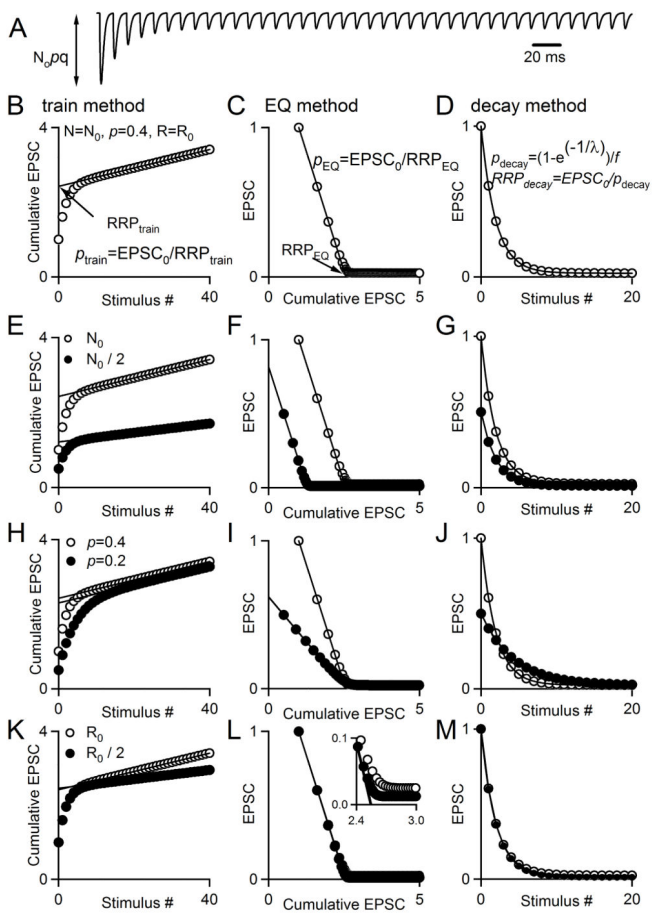

Fig. 1. Using synaptic responses evoked by high-frequency stimulus trains to estimate synaptic parameters

Synaptic responses are described by N_0 (the size of the readily releasable pool, RRP), p (the probability of release), R (the rate of replenishment of the RRP from a reserve pool) and q (the size of a quantal response). **A.** Simulated EPSCs in response to a 100 Hz stimulus train. **B, C.** Two extrapolation methods commonly used to estimate synaptic parameters are illustrated: one referred to as the train method (**B**) and the other as the Elmqvist and Quastel (EQ) method (**C**). **D.** If depression of synaptic responses is due to RRP depletion, the dependence of the EPSC amplitude on number of stimuli can be used to estimate p. **E–G.** The effects of halving N_0 are shown for the train method (**E**), EQ method (**F**), and decay method (**G**). **H–I.** The effect of halving p on the plots used for the train method (**H**), EQ method (**I**), and decay method (**J**). **K–M.** The effect of halving R on the plots used for the train method (**K**), EQ method (**L**), and decay method (**M**).

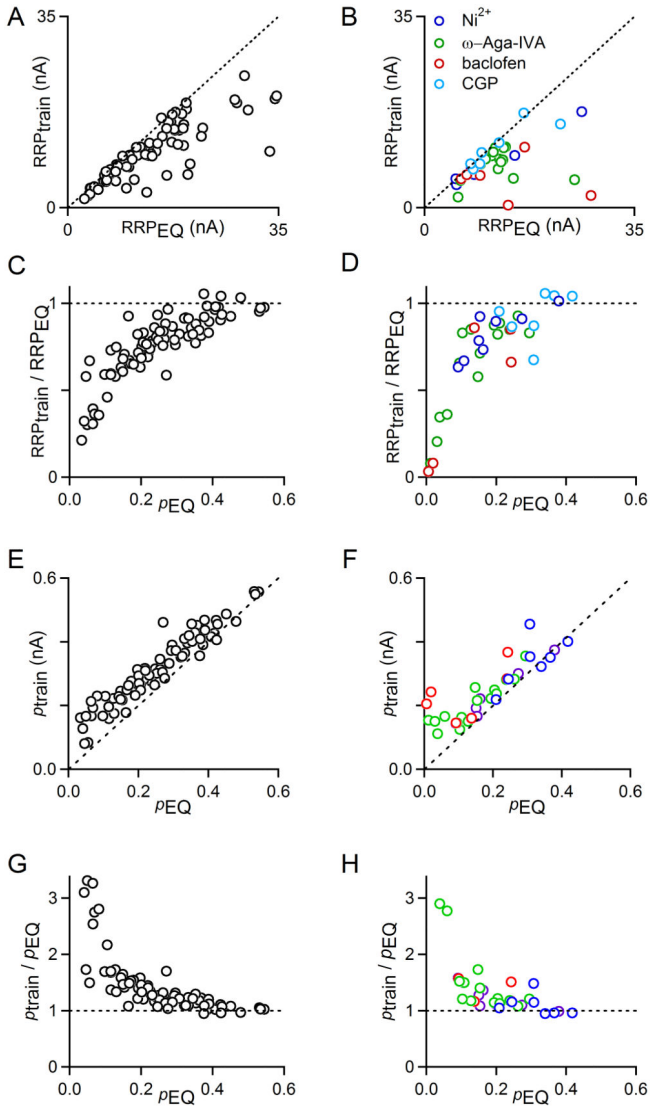

Fig. 2. Linear extrapolation methods provide different estimates of RRP and *p*

EPSCs were evoked with 100 Hz stimulus trains and the train and EQ methods were applied as in Fig. 1B and Fig 1C. In **A**, **C**, **E**, **G**, experiments were performed in different Ca_e (1, 1.25, 1.5, 2, 3, and 4 mM; n=79). In **B**, **D**, **F**, **H**, experiments were performed in the presence of the calcium channel antagonists nickel (Ni; n=8), ω-Aga-IVA (Aga; n=16), the $GABA_B$ receptor agonist baclofen (Bac; n=6) or the $GABA_B$ receptor antagonist CGP 55845 (CGP; n=7). **A.** Comparison of RRP_{train} to RRP_{EQ} for varying Ca_e. Dashed line is the unity line. **B.** Comparison of RRP_{train} to RRP_{EQ} in the presence of Ni (blue circles), Aga (green circles), Bac (red circles), and CGP (light blue circles). Dashed line is the unity line. **C.** Comparison of RRP_{train} divided by RRP_{EQ} as a function of p_{EQ} in varying Ca_e. Dashed line is y=1. **D.** Comparison of RRP_{train} divided by RRP_{EQ} as a function of p_{EQ} in the presence of Ni (blue circles), Aga (green circles), Bac (red circles), and CGP (light blue circles). Dashed line is y=1. **E.** Comparison of p_{train} to p_{EQ} for varying Ca_e. Dashed line is the unity line. **F.** Comparison of p_{train} to p_{EQ} in the presence of Ni (blue circles), Aga (green circles), Bac (red

circles), and CGP (light blue circles). Dashed line is the unity line. **G.** Comparison of p_{train} divided by p_{EQ} as a function of p_{EQ} in varying Ca_e. Dashed line is y=1. **H.** Comparison of p_{train} divided by p_{EQ} as a function of p_{EQ} in the presence of Ni (blue circles), Aga (green circles), Bac (red circles), and CGP (light blue circles). Dashed line is y=1.

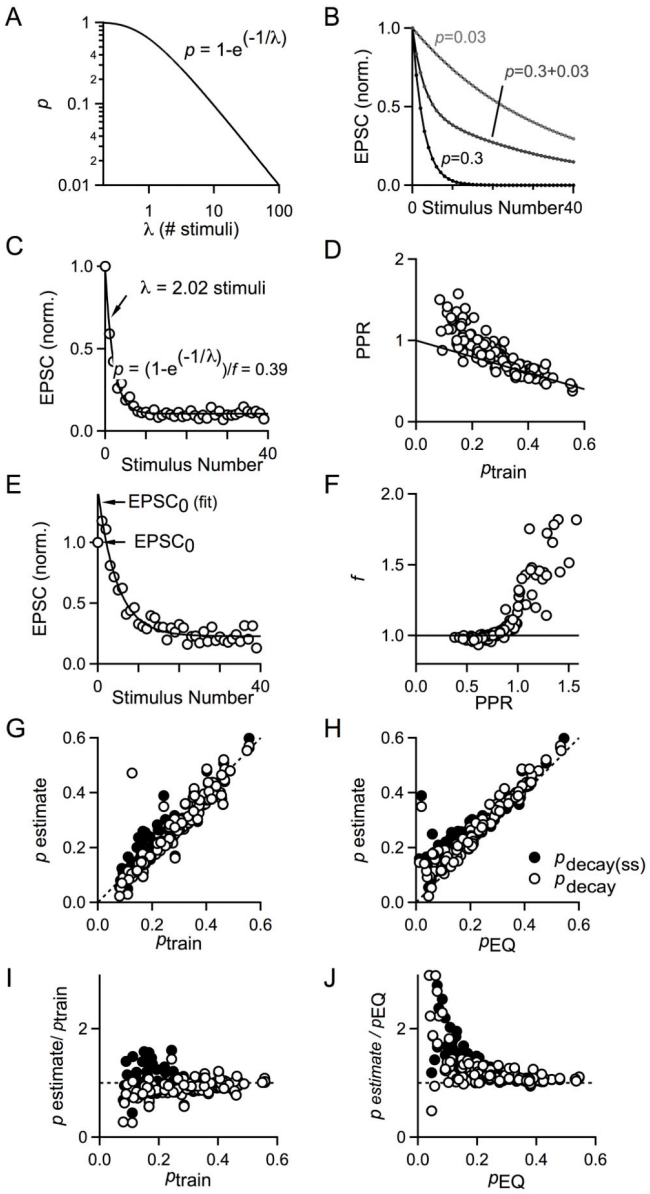

Fig. 3. A direct estimate of p and its comparison to p_{train} and p_{EQ}

A. Plot of the relationship between initial release probability (p) and decay constant λ for a single pool of vesicles according to the equation $p=1-e^{(-1/\lambda)}$. **B.** Plot of EPSC amplitudes simulated for a hypothetical synapse with one pool of vesicles with a single release probability (light gray, black) or two (dark gray) pools of vesicles with different release probabilities which each comprise 50% of the total RRP. For light gray symbols and curve, p=0.03; for dark gray symbols and curve, p_1=0.3 and p_2=0.03; and for black symbols and curve, p=0.3. **C.** Plot of EPSC amplitudes versus stimulus number for 100 Hz stimulus train with single exponential curve fit. The decay constant λ is 2.02 stimuli and can be used to estimate the probability of release**. D.** Plot of PPR vs p_{train} for experiments performed in varying Ca_e and in pharmacological manipulations of calcium entry (n=121). Dotted line corresponds to $1-p$. **E.** A factor, f, was used to account for facilitation between the first and

second action potentials. $p_{\mathbf{decay}} = p_{\mathrm{decay(ss)}}/f$. **F.** Plot of the facilitation factor, f, versus PPR for experiments performed in varying Ca_e and in pharmacological blockers to manipulate calcium entry (n=121). **G**. Plot of $p_{\mathbf{decay}}$ (open circles) and the uncorrected $p_{\mathrm{decay(ss)}}$ (black circles) versus p_{EQ}. Dashed line indicates the unity line, n=122. **H**. Plot of $p_{\mathbf{decay}}$ (open circles) and the uncorrected $p_{\mathrm{decay(ss)}}$ (black circles) versus p_{train}. Dashed line is the unity line. **I.** Plot of $p_{\mathbf{decay}}$ (open circles) and the uncorrected $p_{\mathrm{decay(ss)}}$ (black circles) normalized to p_{train} versus p_{train}. Dashed line is the unity line, n=122. J. Plot of $p_{\mathbf{decay}}$ (open circles) and the uncorrected $p_{\mathbf{decay(ss)}}$ (black circles) normalized to p_{EQ} as a function of p_{EQ}. Dashed line is the unity line, n=107.

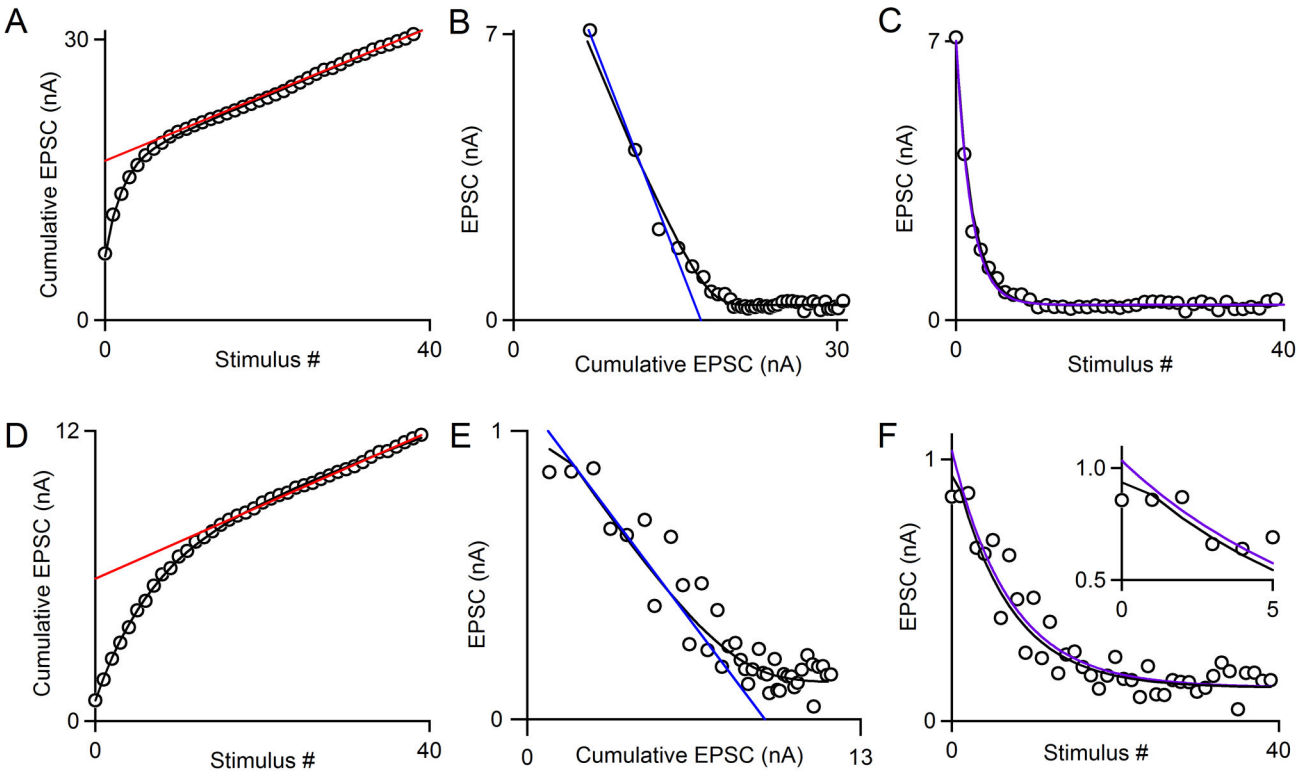

Fig. 4. Comparison of the train, EQ, and decay methods to the NpRf method

A–C. An example of a high p synapse (p_{NpRf} = 0.38). Raw data from synaptic responses to a single stimulus train in an example cell is shown (open circles). **A.** The NpRf method's fit to data is shown (black curve). A fit to the final fifteen points of the cumulative EPSC as is used for the train method is shown (red line). **B.** The NpRf method's fit to data is shown (black curve). A fit to the first four points of the data as is used for the EQ method is shown (blue line). **C.** The NpRf method's fit to data is shown (black curve). A single-exponential fit to all forty points as is used in the decay method for PPR<1 is shown (purple curve). **D–F.** An example of a low *p* synapse (p_{NpRf} = 0.10) and the estimation of synaptic parameters. Raw data from synaptic responses to a single stimulus train in an example cell is shown (open circles). **D.** The NpRf method's fit to data is shown (black curve). The train method is shown (red line). **E.** The NpRf method's fit to data is shown (black curve). A fit to the second through fifth points of the data as is used for the EQ method is shown (blue line). **F.** The NpRf method's fit to the data (black curve) and single-exponential fit to the second through fortieth point as is used in the decay method for PPR>1 (purple curve).

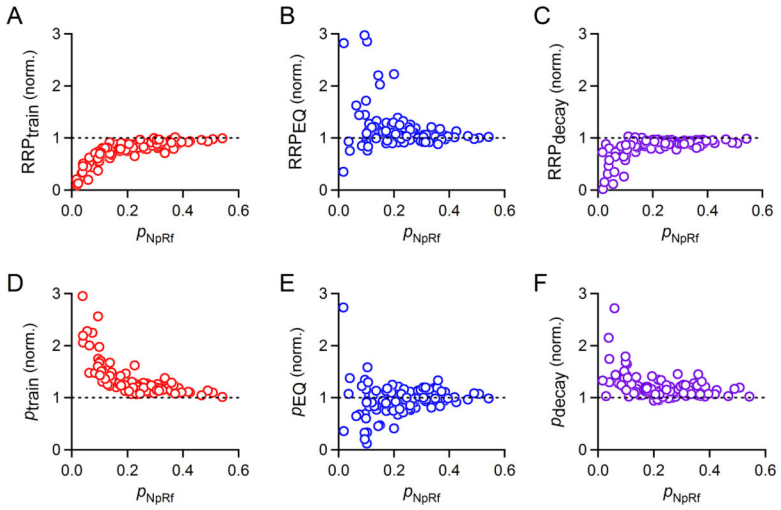

Fig. 5. Performance of a simple depletion model in comparison to train, EQ, and decay methods

Data from many cells stimulated with 100 Hz trains in various recording conditions (same dataset as Figs. 2 and 3). **A.** Plot of RRP_{train} normalized to RRP_{NpRf} as a function of p_{NpRf}, n=122. **B.** Plot of RRP_{EQ} normalized to RRP_{NpRf} as a function of p_{NpRf}, n=107. **C.** Plot of RRP_{decay} normalized to RRP_{NpRf} as a function of p_{NpRf}, n=121. **D.** Plot of p_{train} normalized to p_{NpRf} as a function of p_{NpRf}, n=122. **E. d**Plot of p_{EQ} normalized to p_{NpRf} as a function of p_{NpRf}, n=107. **F.** Plot of p_{decay} normalized to p_{NpRf} as a function of p_{NpRf}, n=121.

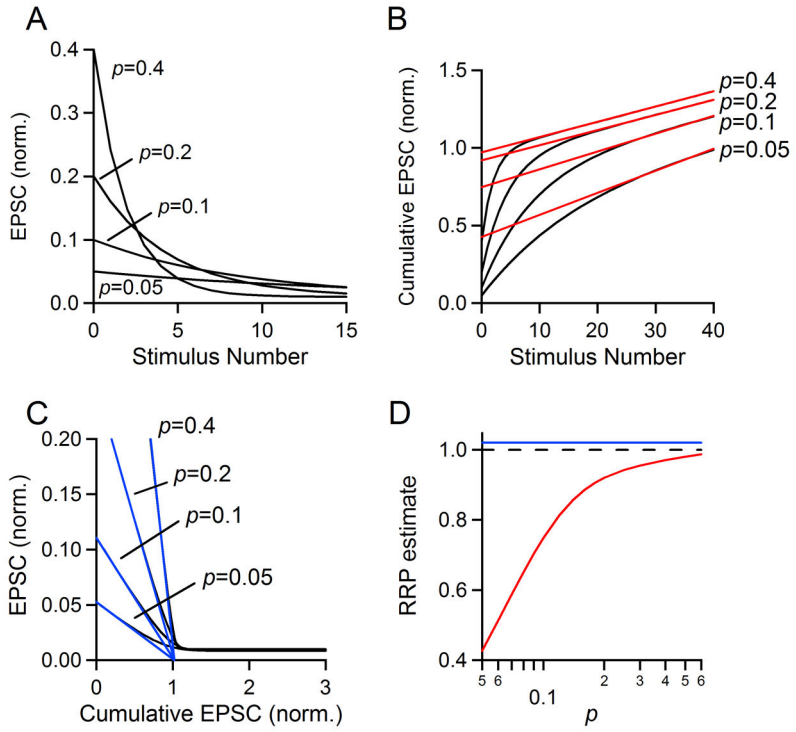

Fig. 6. Effect of changing *p* on estimates of RRP size

A–C. Simulations were performed with $N_0 = 1$, $R = 0.01$ and $p = 0.4$, 0.2, 0.1, or 0.05. **A.** EPSC amplitudes are plotted as a stimulus number for the first 15 stimuli. **B.** The final fifteen points of the cumulative EPSC were fit with a line and back-extrapolated to the y axis to estimate RRP_{train}. **C.** The first four EPSCs were fit with a line and extrapolated to the x axis to estimate RRP_{EQ}. **D.** Simulations were run as in A–C ($N_0 = 1$, R = 0.01) but for a more complete range of values of *p*. RRP estimate as a function of frequency for the train method (red curve) and EQ method (blue line). The actual pool size is equal to one and indicated with a dashed black line.

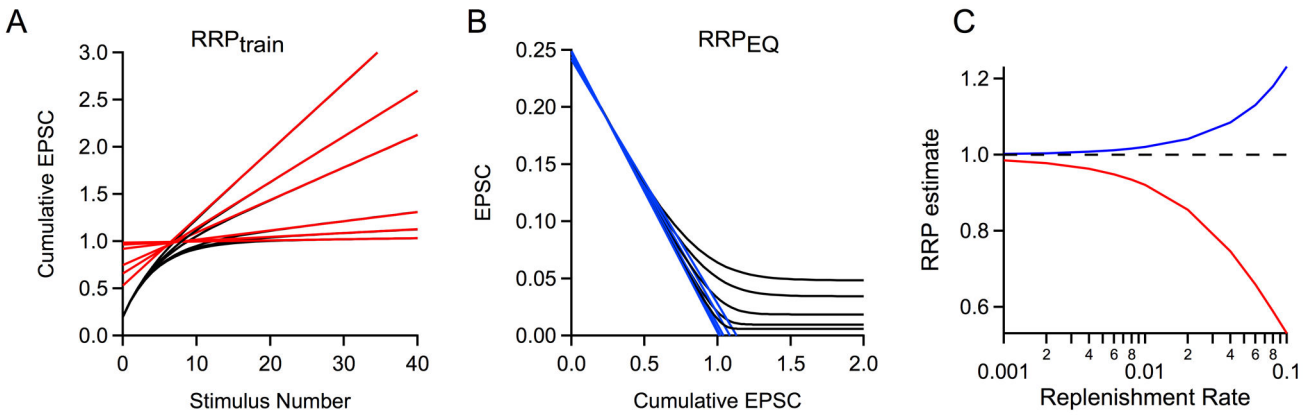

Fig. 7. Effect of changing replenishment rate on the estimated RRP size

A. Simulations were performed using the variables N_0, p, and R values of {1, 0.2, R}, *where* R varies from 0.001 to 0.1. The last fifteen points of cumulative EPSCs were fit with a line and backextrapolated to x=0 to measure RRP_{train}. **B.** Plots of the simulated EPSC amplitude versus cumulative EPSC are shown. Linear fits to the first four points of each curve are extended to y=0, indicating the value of RRP_{EQ}. **C.** The measured pool size as a function of replenishment rate for two methods of RRP estimation: RRP_{train} (red) and RRP_{EQ} (blue). The actual RRP size is equal to one (dotted black line).

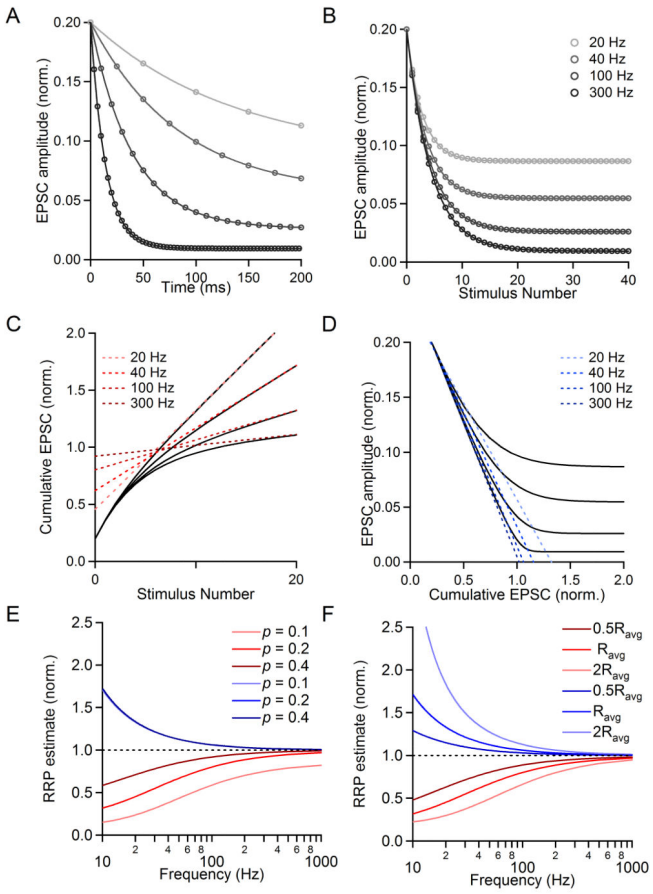

Fig. 8. Effect of changing stimulus frequency on the estimated RRP size

Simulations were performed using the variables N_0, p, and R values of {1, 0.2, R}. The value of R was changed to simulate firing at different frequencies, and was determined from our characterization of recovery from depression (see text for details). The frequencies shown are 20 Hz, 40 Hz, 100 Hz, and 300 Hz. **A.** EPSC amplitude (normalized to RRP size) versus time shown for simulations at different frequencies. **B.** Plots of EPSC size (norm. to RRP size) versus stimulus number. **C.** The last fifteen points of cumulative EPSCs were fit with a line and backextrapolated to x=0 to measure RRP_{train}. **D.** Plots of the simulated EPSC amplitude versus cumulative EPSC are shown. Linear fits to the first four points of each curve are extended to y=0, indicating the value of RRP_{EQ}. **E.** The measured pool size as a function of frequency for two methods of RRP estimation: RRP_{train} (red) and RRP_{EQ} (blue) for different values of p. The actual RRP size is equal to one (dashed black line). **F.** The measured pool size as a function of frequency as shown before for different replenishment rates (R=0.0295). The actual RRP size is equal to one (dotted black line).

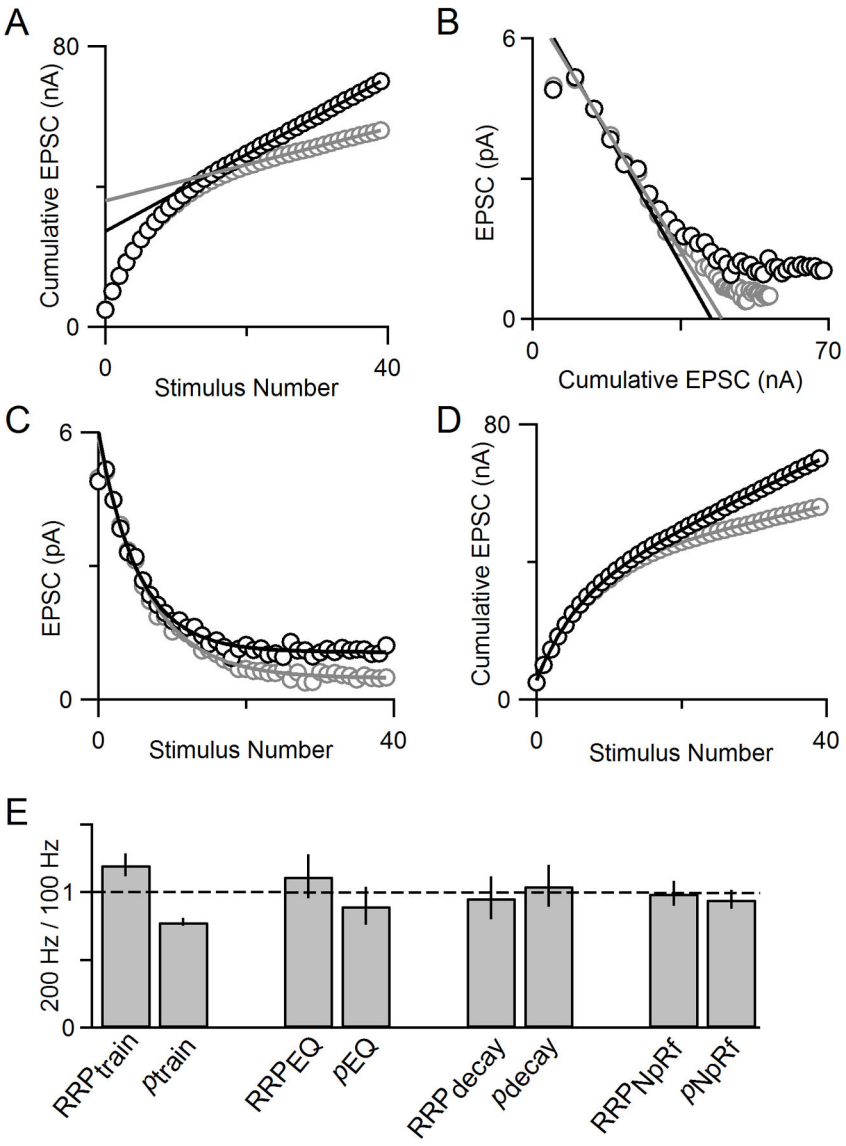

Fig. 9. Comparison of 4 methods for different stimulus frequencies

A. Cumulative EPSC plotted for an example cell shows that RRP_{train} is larger for the 200 Hz train (gray) than for the 100 Hz train (black). **B.** EPSC amplitude versus cumulative EPSC shows that RRP_{EQ} is very similar for 100 Hz (black) and 200 Hz (gray) stimulus trains in an example cell. **C.** EPSC amplitude versus stimulus number for 100 Hz and 200 Hz trains in an example cell with single exponential fits (solid curves) according to the decay method. **D.** Cumulative EPSCs with model fits plotted for 100 Hz (data shown as gray open circles and model fit as a gray line) and 200 Hz (data shown as black open circles and model fit as a black line) can be used to estimate RRP size. **E.** Summary data for all four techniques of measuring RRP size (n=4).

Table 1

Summary of methods for estimating parameters of synaptic transmission.

Method	**train**	**EQ**	**decay**	**decay(ss)**	**NpRf**
Figures	1–9	1–9	3–5, 9	3	4–9
RRP size	RRP_{train}	RRP_{EQ}	RRP_{decay}	$RRP_{decay(ss)}$	RRP_{NpRf}
p	p_{train}	p_{EQ}	p_{decay}	$p_{decay(ss)}$	p_{NpRf}
Replenishment rate	-	0	-	-	R_{NpRf}
Key reference Assumptions	(Schneggenburge r et al., 1999)	(Elmqvist and Quastel, 1965)	(Ruiz et al., 2011)	-	-
Single pool depletion	Yes	Yes	Yes	Yes	Yes
Constant *p* throughout train	No	Yes	Yes	Yes	Yes
Uniform *p* for all vesicles	No	Yes	Yes	Yes	Yes
Constant replenishment	Yes; maximal	Yes; none	Yes	Yes	Constant rate *with respect to proportion of available sites* in RRP